

000 001 002 003 004 005 006 007 008 009 010 011 012 013 014 015 016 017 018 019 020 021 022 023 024 025 026 027 028 029 030 031 032 033 034 035 036 037 038 039 040 041 042 043 044 045 046 047 048 049 050 051 052 053 HOW EFFECTIVE IS YOUR REBUTTAL? IDENTIFYING CAUSAL MODELS FROM THE OPENREVIEW SYSTEM

Anonymous authors

Paper under double-blind review

ABSTRACT

The peer review process is central to scientific publishing, with the rebuttal phase offering authors a critical opportunity to address reviewer concerns. However, the causal mechanisms that determine rebuttal effectiveness, particularly how author responses influence final review decisions, remain poorly understood. In this work, we present a two-layer causal analysis of ICLR submissions from the OpenReview system. At the structured level, we combine metadata features (e.g., soundness, presentation) with LLM-inferred features (e.g., clarity, directness), and apply independence tests to identify their associations with rating changes. At the unstructured level, we model rebuttal texts using a weakly supervised Causal Representation Learning (CRL) framework, guided by LLM-inferred features as concept-level supervision. Theoretically, we establish identifiability conditions for recovering latent concepts under mild assumptions. Empirically, our analysis uncovers causal patterns across structured and unstructured features, revealing how specific rebuttal strategies shape reviewer assessments. These findings offer actionable guidance for authors in crafting more effective rebuttals and contribute to broader goals of transparency, fairness, and efficiency in peer review processes.

1 INTRODUCTION

Peer review is the cornerstone of scientific progress, ensuring rigor, reliability, and integrity in published research (Tennant, 2018; Alberts et al., 2008; Tennant & Ross-Hellauer, 2020; Ceci & Peters, 1982). In recent years, the machine learning community has advanced transparency by adopting platforms like OpenReview, where reviews, author responses (rebuttals), and ratings are openly available (Tran et al., 2020; Wang et al., 2023a; Sun et al., 2025a; Ross-Hellauer, 2017). This openness presents a rare opportunity to examine how rebuttals influence reviewer judgement, a process often considered important yet poorly understood. Despite its significance, we still lack systematic evidence on what makes rebuttals persuasive and what strategies impact reviewers' ratings.

Prior work on peer review has investigated systemic properties such as bias (Tomkins et al., 2017), arbitrariness (Langford & Guzdial, 2015), predictive validity (Ragone et al., 2013; Wolfram et al., 2020), and integrity (Barrière et al., 2023). Analyses of OpenReview data have studied reviewer behavior and rating consistency (Stelmakh et al., 2021; Gao et al., 2019), while controlled trials examined anchoring effects in scoring (Liu et al., 2024). Several studies have examined the role of rebuttals in the review process. For instance, Shah et al. (2018) found limited score shifts after rebuttal despite active discussion, while Huang et al. (2023) analyzed ICLR 2022 reviews and identified social interaction structures and author strategies that contribute to successful rebuttals. In parallel, Wu et al. (2022) incorporated rebuttal counter-arguments into meta-review generation. However, existing research remains correlational and descriptive, leaving open the causal question of why and how some rebuttal strategies succeed. Please refer to App. A3 for more details about the related work.

Building on the limitations of prior correlational studies, we analyze 8684 ICLR 2024–2025 submissions from the OpenReview system to uncover the causal factors driving score changes. Our analysis consists of two progressive layers. First, we analyze structured features. We construct 24 tabular features, including 8 review-level features (e.g., soundness, presentation), 6 paper-level features (e.g., abstract length), and 10 higher-level LLM-inferred features, which we also refer to as *concepts* (e.g., clarity, directness). These concepts are designed to capture human-aligned signals of rebuttal effectiveness, though they may be noisy or imperfect. To assess their relationship with rating changes,

054
 055 **Table 1: Dataset statistics of ICLR 2024 and 2025 with paired ratings (initial and final) from**
 056 **Paper Copilot Yang (2025).** The table reports paper-level statistics and review-level statistics.

	Paper Statistics						Review Statistics		
	Poster	Spotlight	Oral	Reject	Withdraw	Total	Reviewed Papers	Avg. Reviews/Paper	Total Reviews
ICLR'24	1321	290	61	1287	127	3086	3086	3.9	12035
ICLR'25	2412	306	172	2409	252	5598	5598	4.1	22951
Total	3733	596	233	3696	379	8684	8684	4.0	35033

061
 062
 063 we apply five conditional independence tests: KCI (Zhang et al., 2012), RCIT (Strobl et al., 2019),
 064 HSIC (Gretton et al., 2005), Chi-square (Tallarida et al., 1987), and G-square (Tsamardinos et al.,
 065 2006). Second, we extend the analysis with textual causal representation learning (CRL). Rather
 066 than relying only on predefined, noisy LLM-inferred *concepts*, we aim to directly recover latent
 067 *concepts* from rebuttal and review text. This second layer serves two purposes. First, it corrects for
 068 the noise and potential biases in the LLM-inferred *concept* by learning representations that more
 069 closely reflect the underlying causal factors. Second, it adds new *concepts* beyond our predefined
 070 set, uncovering dimensions of rebuttal effectiveness that may not be anticipated by human intuition.
 071 Recent advances in CRL enable the identification of interpretable *concepts* from high-dimensional
 072 text (Schölkopf et al., 2021; Yao et al., 2024), especially when supported by weak supervision
 073 with *concept* cues (Rajendran et al., 2024; Locatello et al., 2020) and variation induced by multiple
 074 distributions or interventions (Zhang et al., 2024; Ahuja et al., 2023). In this way, CRL builds directly
 075 on the structured analysis, refining noisy *concept* features while also discovering new latent *concepts*,
 thereby providing a richer understanding of how rebuttal strategies shape reviewer assessments.

076 To summarize, our contributions are twofold. First, we conduct a deep and wide-ranging analysis of
 077 rebuttal effectiveness across structured features, covering paper-level metadata, review-level features,
 078 and LLM-inferred *concepts*. By applying established independence tests in this setting, we provide a
 079 comprehensive examination and extract insightful patterns about which factors are dependent from
 080 rating changes. Second, we frame rebuttal effectiveness as a causal modeling problem and situate
 081 it within a multi-distribution framework. Building on this formulation, we introduce a new causal
 082 model and establish novel identifiability results for recovering latent *concepts* from rebuttal and
 083 review text. These two layers are progressive: the structured layer offers weak supervision to guide
 084 CRL, while CRL both refines noisy concepts and uncovers additional ones beyond the predefined
 085 set. Together, these contributions advance the theoretical foundations and empirical understanding of
 086 rebuttals, while offering practical guidance for crafting more effective responses in OpenReview.

087 2 DATASETS

090 **Data Collection and Processing.** We build on data from Paper Copilot (Yang, 2025), a website
 091 launched two years ago to aggregate and analyze AI conference data. Since 2024, Paper Copilot
 092 has compiled peer review records from major conferences, and for ICLR it provides both initial
 093 and final reviewer ratings. We focus on ICLR 2024 and 2025 submissions because they not only
 094 include these paired ratings, which are crucial for analyzing rating changes, but also offer the most
 095 complete author–reviewer discussion records available in the OpenReview system. In contrast, other
 096 conferences in Paper Copilot often release only final ratings, making it impossible to study rating
 097 changes. Our dataset includes reviews, rebuttals, and subsequent discussions. In total, we collect 8696
 098 papers, with additional statistics reported in Tab. 1. To ensure fair and meaningful analysis, we filter
 099 out papers without rebuttals. After processing, we obtain 23922 valid reviewer–author discussion
 100 samples, each with paired ratings. This dataset provides sufficient scale for both independent test and
 101 CRL, enabling us to study rebuttal effectiveness from complementary perspectives.

102 **Metadata Features.** Each paper is typically evaluated by multiple reviewers, so we collect 8
 103 review-level features (*initial confidence*, *final confidence*, *confidence change*, *number of interactions*,
 104 *soundness*, *presentation*, *contribution*, and the average of other reviewers' initial ratings) and 6
 105 paper-level features (*submission number*, *title length*, *abstract length*, *number of authors*, *status*, and
 106 *primary area*). Here, the number of interactions denotes how many rounds of discussion occur
 107 between the author and a reviewer. The feature average of other reviewers' initial ratings is designed
 to capture how peer assessments may influence an individual reviewer. Together, these metadata

108

109 Table 2: **Comparison of LLMs in scoring concept features.** We report the L_2 norm between
 110 LLM predictions and human annotations for 10 concept features: *Clarity (CL)*, *Directness (DI)*,
 111 *Attitude (AT)*, *Author Openness (AO)*, *Evidence (EV)*, *Rigor (RI)*, *De-Escalation (DE)*,
 112 *Specificity and Constructiveness (SC)*, *Reviewer Openness (RO)*, and *Concern Severity (CS)*. The final column
 113 shows the average L_2 error (AE) across all features, and *TC* denotes the average time cost.

Models (LLMs)	Metrics											
	TC↓	CL↓	DI↓	AT↓	AO↓	EV↓	RI↓	RI↓	SC↓	RO↓	CS↓	AE↓
DeepSeek-R1	18.33s	0.30	0.55	0.47	0.60	0.83	0.63	0.67	0.80	0.55	0.80	0.62
Grok-3-Latest	11.74s	0.45	0.50	0.74	0.60	0.39	0.53	0.67	1.00	0.90	1.30	0.71
Gemini-2.0-Flash-Lite	3.70s	0.40	0.75	0.53	0.95	0.89	0.58	1.00	0.30	1.10	0.65	0.71
ChatGPT-4.1-Mini	9.73s	0.35	0.65	0.95	0.95	0.94	0.63	1.00	1.25	0.60	0.65	0.80
Gemini-2.0-Flash	4.12s	0.45	1.10	0.79	0.95	1.11	0.74	0.83	0.75	1.05	0.45	0.82
ChatGPT-4.1	9.73s	0.55	0.70	0.79	1.05	0.89	0.84	0.67	1.40	0.90	0.65	0.84
ChatGPT-4.1-Nano	5.34s	0.35	0.55	1.05	1.30	0.72	0.58	2.50	0.50	0.50	0.75	0.88
Llama-4-Maverick	5.86s	0.50	0.75	1.26	1.35	1.28	0.89	2.00	0.75	0.70	0.75	1.02
Gemini-2.5-Flash-Preview-04-17	13.26s	0.65	0.75	0.74	1.35	0.94	0.84	1.17	1.45	1.20	1.25	1.03
Deepseek-V3-0324	5.94s	0.55	1.00	1.84	0.80	1.28	1.16	1.50	1.40	1.30	0.85	1.17
ChatGPT-4o-Latest	8.43s	0.60	1.30	2.00	1.40	1.17	0.95	2.17	2.00	1.05	0.80	1.34

124
 125 features reflect both the content and dynamics of the peer review process. The App. A4.2 and App. A2
 126 present a full description of all features and their distributions respectively. Together, these features
 127 serve as the foundation for our structured analysis.
 128

129 **LLM-Inferred Features.** To capture finer-grained aspects of rebuttals and reviews, we introduce
 130 ten human-interpretable features, hereafter referred to as *concepts*. Seven are author-related: *clar-
 131 ity*, *directness*, *attitude*, *openness*, *evidence*, *rigor*, and *de-escalation*. Three are reviewer-related:
 132 *specificity and constructiveness*, *openness*, and *concern severity*. Formal definitions and empirical
 133 distributions of these features are provided in App. A4.1 and App. A1. All features are annotated
 134 on a five-point ordinal scale. To scale annotation beyond manual labeling, we benchmarked several
 135 LLMs on a randomly sampled set of 200 annotated examples (20 rebuttals evaluated across 10
 136 features). Each example was independently labeled by two senior machine learning researchers,
 137 with disagreements resolved through discussion to produce gold-standard scores. We then compared
 138 LLM-inferred predictions against expert annotations using the L_2 norm.

139 The results in Tab. 2 show that DeepSeek-R1 achieves the best overall alignment with human
 140 annotations, with the lowest average L_2 error across all concept features, albeit at a rather costly
 141 inference time. Grok-3-Latest and Gemini-2.0-Flash-Lite perform competitively (av-
 142 erage error 0.71) while being faster, but with higher variance across specific features. In contrast,
 143 models such as ChatGPT-4o-Latest and DeepSeek-V3-0324 exhibit significantly larger
 144 errors (>1.0), indicating weaker consistency with expert labels. Overall, DeepSeek-R1 providing
 145 the best performance for large-scale inference. Based on this result, we adopt DeepSeek-R1 for
 146 large-scale inference. Due to budget and inference time constraints, we annotate a 10% subset of the
 147 dataset (2393 samples) using DeepSeek-R1. The full prompt is provided in Prompt 1 and 2.
 148

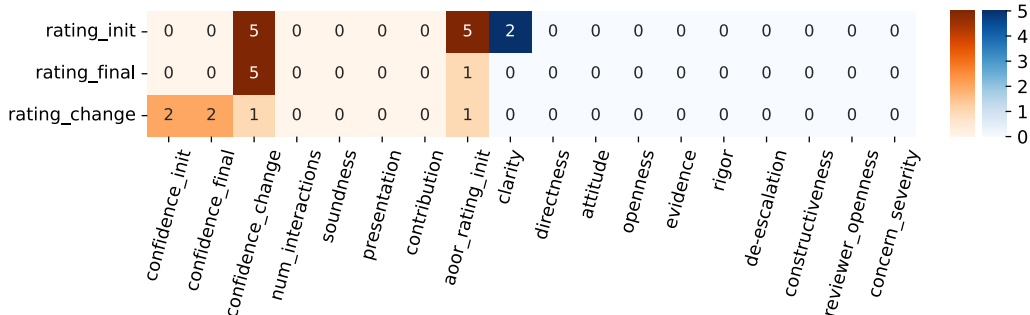
149 3 FIRST LAYER: STRUCTURED FEATURE ANALYSIS

150 To identify which factors influence reviewer ratings, we investigate how review- and rebuttal-related
 151 features are associated with rating changes. For this purpose, we apply five widely used independence
 152 tests: KCI (Zhang et al., 2012), RCIT (Strobl et al., 2019), HSIC (Gretton et al., 2005), Chi-square
 153 (Tallarida et al., 1987), and G-square (Tsamardinos et al., 2006). The tests are conducted on two sets
 154 of features: (i) 14 metadata features available for all 23922 reviewer–author discussions, and (ii) the
 155 annotated subset (2393 samples) with 10 LLM-inferred features. At the review level, Fig. 1 reports
 156 the aggregated independence test results between ratings and metadata or LLM-inferred features.
 157 At the paper level, Fig. 2 shows the aggregated results between the average paper rating and the
 158 six paper-level metadata features. Together, these analyses provide a comprehensive view of how
 159 different types of features may be linked to changes in reviewer ratings.
 160

161 **Analysis of review-level metadata features.** As shown in Fig. 1 (orange), for both initial and final
 162 ratings, we find strong dependence on core review attributes such as *soundness*, *presentation*, and

162
163
164
165
166

Figure 1: **Aggregated independence test results** between rating and metadata features (orange) or LLM-inferred features (blue). Each cell reports how many of the five tests fail to reject independence at significance level $\alpha=0.05$. A value of 0 indicates strong evidence of dependence, while 5 indicates strong evidence of independence across all tests. Refer to Fig. A5.2-A5 for all complete p values.

167
168
169
170
171
172
173
174
175
176177
178
179
180
181
182
183
184

contribution. This pattern is consistent across all five tests, indicating that these factors reliably shape how reviewers assign scores. Interestingly, *rating_init* and *rating_final* appear independent of each other but both are dependent on *rating_change*, suggesting that absolute ratings and their shifts capture complementary aspects of the review process. Rating changes show weaker but notable dependence on *initial/final confidence* and on the *average of other reviewers' initial ratings*, highlighting the role of confidence and peer influence in shaping score adjustments. Finally, the *number of interactions* also exhibits dependence with *rating_change*, underscoring the importance of active reviewer–author engagement during the discussion phase.

185
186
187
188
189
190
191
192
193
194
195
196
197
198

Analysis of LLM-inferred features. Also in Fig. 1 (blue), turning to the ten concept features extracted from rebuttal and review text, we observe systematic dependence with rating changes. Features such as *clarity*, *directness*, *attitude*, *openness*, *evidence quality*, and *rigor* all show strong associations with score adjustments, suggesting that the style and substance of rebuttals are key drivers of reviewer updates. Unlike review-level metadata, which primarily governs baseline ratings, these content-oriented concepts appear to capture how authors' responses shift reviewers' perceptions. This supports the intuition that rebuttal effectiveness is closely tied to the persuasiveness and tone of the exchange.

199
200
201
202
203
204
205
206
207
208
209
210

Analysis of paper-level metadata features. As shown in Fig. 2, static paper descriptors such as *title length*, *abstract length*, *number of authors*, and *primary area* exhibit little evidence of association with rating changes. In most cases, the tests fail to reject independence, particularly for average rating adjustments, indicating that these surface-level attributes have minimal impact on how scores evolve during the rebuttal stage. Weak dependencies are observed for *submission number*, *abstract length*, and *number of authors* with initial ratings, but these effects vanish once rating changes are considered. This suggests that while such metadata may weakly shape first impressions, it does not determine whether reviewers subsequently adjust their scores. Taken together, these findings underscore an important distinction: paper-level descriptors capture static characteristics of the submission, but rebuttal effectiveness hinges on dynamic interactions between authors and reviewers. In other words, what changes minds is not how long the title is or how many co-authors are listed, but rather the persuasiveness, clarity, and responsiveness demonstrated during the rebuttal process.

211
212
213
214
215

Takeaway. Our findings have several insights for the machine learning community. We highlight that rebuttal effectiveness depends more on discourse quality than on paper metadata. For authors, features such as *clarity*, *rigor*, *evidence*, and *constructiveness* are most associated with rating gains, whereas *soundness*, *presentation*, *contribution*, and *confidence* measures show little effect (see Fig. 3). For reviewers and area chairs, this underscores the need for calibration, as specific rebuttal strategies can systematically shape score adjustments. We also observe a regression-to-the-mean

Figure 2: **Aggregated independence test results** between average rating and paper-level metadata features.

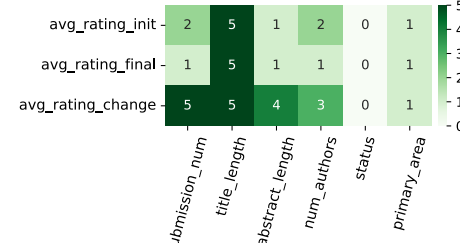
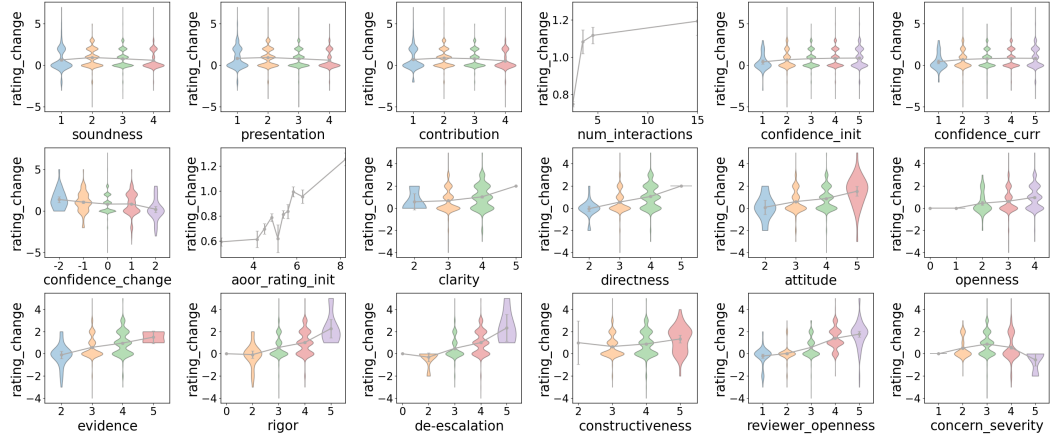


Figure 3: **Dependency panels of rating changes and various features.** Each subplot shows the distribution of rating_change conditioned on metadata or LLM-inferred features. Most features are centered around zero, indicating little systematic effect. Notable dependencies appear for *aoor_rating_init* (lower initial ratings linked to positive changes, consistent with a regression-to-the-mean effect), *num_interactions* (more exchanges associated with slight gains), and discourse-related features such as *clarity*, *rigor*, *evidence*, and *constructiveness*, which show modest positive shifts. Appendix A6 provide the corresponding dependency panels for *rating_init* and *rating_final*.

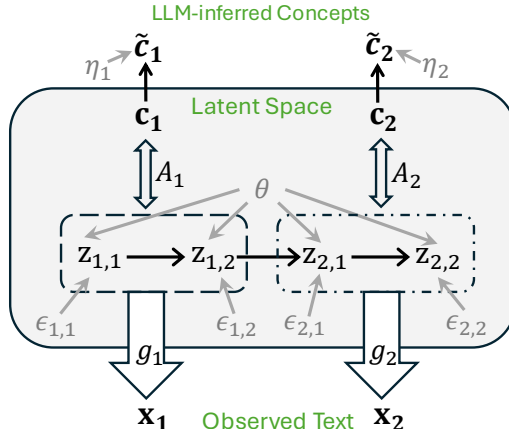


effect, where lower initial ratings tend to increase, and a modest positive trend with more reviewer-author interactions. Overall, the substance and quality of rebuttals matter in influencing final rating.

4 SECOND LAYER: HUMAN-ALIGNED CAUSAL REPRESENTATION LEARNING

Beyond structured metadata features, rebuttals involve high-dimensional textual interactions between reviewers and authors. To move beyond predefined and potentially noisy features, we employ causal representation learning (CRL) (Xu et al., 2024; Zheng et al., 2022; Yao et al., 2023; Sun et al., 2025b). These two layers are progressive: the structured feature analysis in the previous section provides weak supervision for CRL, while CRL serves two complementary functions. First, it refines noisy LLM-inferred concepts by recovering latent representations that better align with the true underlying concepts. Second, it uncovers additional human-aligned concepts beyond the predefined set, capturing aspects of rebuttal effectiveness that may not be immediately apparent. Our setting naturally exhibits multiple modalities (reviewer text and author text) and heterogeneous distributions (e.g., different primary areas, reviewer backgrounds), which provide the variation necessary for causal identification. Fig. 4 illustrates that the causal model of the rebuttal process with two modalities. We organize this section as follows. In § 4.1, we introduce our causal formulation, motivated by the real-world rebuttal problem. § 4.2 develops the identifiability theory grounded in this formulation. Building on these insights, § 4.3 presents our network design and training procedure. To evaluate the effectiveness of the proposed method, we conduct synthetic experiments in § 4.4. Finally, § 4.5 applies our approach to the rebuttal dataset, providing the actionable insights and practical guidance on effective rebuttal strategies.

Figure 4: **Causal model of the rebuttal process with two modalities**, capturing latent factors from reviewers (\mathbf{z}_1) and authors (\mathbf{z}_2). The framework allows bidirectional causal influences between \mathbf{z}_1 and \mathbf{z}_2 , reflecting the interactive nature of rebuttal discussions. \mathbf{x} denotes the observed text, \mathbf{c} the true human-aligned concepts, and $\tilde{\mathbf{c}}$ the noisy estimation inferred by LLMs used as weak supervision.



270 4.1 CAUSAL FORMULATION
271

272 We denote the observed text as $\mathbf{x} = [\mathbf{x}_1, \mathbf{x}_2]$, where \mathbf{x}_1 represents aggregated reviewer text and \mathbf{x}_2
273 aggregated author text. These are generated from latent variables $\mathbf{z} = [\mathbf{z}_1, \mathbf{z}_2]$, which capture hidden
274 factors underlying how reviewers and authors express themselves, respectively. We introduce θ to
275 represent the heterogeneity of latent variables across different primary areas or reviewer backgrounds.
276

277 On top of the latent variables, we define a set of human-aligned concepts $\mathbf{c} = [\mathbf{c}_1, \mathbf{c}_2]$, which corre-
278 spond to interpretable attributes such as *openness*. Each concept is modeled as a linear projection of \mathbf{z}
279 through a mapping A . In practice, however, LLMs-inferred scores only provide noisy approximations
280 $\tilde{\mathbf{c}}$ of these concepts, which we generally represent this relation as $\tilde{c}_{m,i} = c_{m,i} + \eta_{m,i}$, where η are
281 Gaussian noises introduced by annotation variability, prompt ambiguity, or model bias.
282

283 Formally, the data-generating process of the variables defined above can be written as:
284

$$z_{m,i} := h_{m,i}(\text{Pa}(z_{m,i}), \theta, \epsilon_{m,i}), \quad \text{(latent causal relations)} \quad (1)$$

$$\mathbf{x}_m := g_m(\mathbf{z}_m), \quad \text{(observed text)} \quad (2)$$

$$\mathbf{c}_m := A \mathbf{z}_m, \quad \text{(true human-aligned concepts)} \quad (3)$$

$$\tilde{c}_{m,i} := c_{m,i} + \eta_{m,i}, \quad \text{(noisy concepts inferred by LLMs)} \quad (4)$$

290 where $m \in \{1, 2\}$ indexes reviewers ($m=1$) and authors ($m=2$). $\text{Pa}(z_{m,i})$ are the parents of $z_{m,i}$ in
291 the latent causal graph \mathcal{G}_z , $\epsilon_{m,i}$ are exogenous noise variables, g_m is a nonlinear mixing function
292 mapping \mathbf{z}_m to observed text \mathbf{x}_m , and A is a linear matrix aligning \mathbf{z}_m with human-interpretable
293 concepts \mathbf{c}_m . Notably, we treat the noisy LLM-derived $\tilde{\mathbf{c}}$ as weak supervision for CRL training;
294 ultimately, CRL refines them to recover the true concept \mathbf{c} by utilizing the estimated $\hat{\mathbf{z}}$, thereby
295 offering a more reliable concept representation beyond LLM-inferred results.
296

297 4.2 IDENTIFIABILITY THEORY
298

300 A central question in our setting is whether human-aligned concepts \mathbf{c} can be uniquely recovered
301 from the observational data. More concretely, we are given an observational dataset (all reviews)
302 together with multiple concept-conditional datasets (subsets of reviews filtered by concept scores)
303 with LLM-inferred noisy concept; the fundamental problem is to determine the conditions under
304 which the true underlying concepts can be recovered from them with minor indeterminacy.
305

306 **Definition 1. (Identifiability)** *Given observational and concept-conditional datasets, we say the
307 concepts $\mathbf{c} = \{c^1, \dots, c^m\}$ with associated linear maps $\{A^1, \dots, A^m\}$ are **identifiable** if, for any
308 alternative parameterization $(\tilde{f}, \tilde{A}^e, \tilde{b}^e)$ that produces the same observed data distributions, there
309 exists an invertible linear map T , a shift $w \in \mathbb{R}^{d_z}$, permutation matrices P^e , and invertible diagonal
310 matrices Λ^e such that, for all \mathbf{x} and for each concept e , the concept parameters are related by*
311

$$\tilde{A}^e \tilde{f}^{-1}(\mathbf{x}) = \Lambda^e P^e A^e (f^{-1}(\mathbf{x}) + w), \quad \tilde{A}^e = P^e A^e T^{-1}, \quad \tilde{b}^e = \Lambda^e P^e (b^e - A^e w). \quad (5)$$

312 In this context, *identifiability* means that the human-aligned concepts \mathbf{c} can be recovered up to a small
313 set of unavoidable ambiguities. Specifically, in Eq. 5, the subspaces corresponding to interpretable
314 dimensions such as *soundness* or *clarity* and their evaluation maps can be consistently learned,
315 modulo permutation (P^e), scaling (Λ^e), and a global linear transformation of the latent space (A).
316 These ambiguities are intrinsic to causal representation learning, since the latent variables \mathbf{z} are never
317 directly observed; however, they do not obstruct our objective if we can recover them up to minor
318 indeterminacy. Learning the evaluation maps $A^e f^{-1}$ allows us to dissect rebuttals, identify which
319 latent factors causally drive reviewer perceptions, and align the results with interpretable axes such as
320 rigor, evidence, or openness. Importantly, the conditions for identifiability, relying on the diversity
321 of concept-conditional distributions, are naturally satisfied in our setting due to the rich variety of
322 sub-score data available in the OpenReview System.
323

324
 325 **Theorem 1. (Identifiability of Concepts)** Suppose we match the observations \mathbf{x}_m across modalities
 326 (authors and reviewers), and the following conditions hold in the data-generating process:

327 *i (Information Preservation):* The functions g_1 and g_2 are differentiable and invertible.

328 *ii (Sufficient Diversity):* All entries of $v^\top B$ are non-zero, where $B_{i,j} = \frac{b_k^e}{\sigma^2}$ denotes the
 329 area-concept matrix.

330 *iii (Distinctive Concept Alignment):* There exists a set of linearly independent aligning vectors
 331 $\mathcal{C} = \{a_1, \dots, a_n\}$ such that, for each concept C^e , the rows of the aligning matrix A^e lie in \mathcal{C} ,
 332 i.e., $(A^e)^\top e_i \in \mathcal{C}$. Let S^e denote the indices of the subset of \mathcal{C} that appear as rows of A^e . Every
 333 aligning vector in \mathcal{C} appears in at least one primary area e (where an area corresponds to a
 334 concept-conditional distribution), that is,

$$\bigcup_e S^e = [n].$$

335
 336 *Then the concepts \mathbf{c} are identifiable as demonstrated in Definition 1.*

337
 338 Assumption i requires that the latent space is recoverable from the observed data. Assumption ii
 339 further requires the presence of latent distribution shifts in the review concepts across different
 340 primary areas, ensuring variability in the underlying structure. Finally, Assumption iii ensures that
 341 all concepts can be decomposed into a finite set of atomic components that remain distinct across
 342 primary areas, which is essential. Under such a theorem, we can guarantee that the hidden concepts
 343 are uniquely recovered and aligned with the LLM-inferred noisy version, ensuring the correctness of
 344 the obtained causal relations on those latent embeddings through conditional independence testing.

345 **4.3 NETWORK DESIGN**

346 Building on the identifiability conditions, we now describe our practical framework for learning latent
 347 causal representations from rebuttal and review text. The key challenge is to approximate the posterior
 348 distribution of latent variables \mathbf{z} given observed embeddings \mathbf{x} , while accounting for domain-specific
 349 variation θ (e.g., primary research areas or reviewer backgrounds). Since the generative process
 350 $\mathbf{x} = g(\mathbf{z})$ is highly nonlinear, the posterior $p(\mathbf{z}|\mathbf{x}, \theta)$ is intractable. We therefore adopt a variational
 351 approach enhanced with flow-based priors.

352 Following the general CRL framework (Zhang et al., 2024), we use a Dense Sigmoid Flow (DDSF)
 353 (Wehenkel & Louppe, 2019) to implement the prior distribution over \mathbf{z} . The flow transforms each
 354 dependent latent variable z_i into an independent noise variable ϵ_i , conditioned on its latent parents
 355 and domain factor θ . Let W denote the adjacency matrix of the latent causal graph \mathcal{G}_z , and \hat{W} be the
 356 estimated one. For each \hat{z}_i , the transformation is:

$$\hat{\epsilon}_i, \log \det J_i = \text{Flow}\left(\hat{z}_i; \text{NN}(\{\hat{W}_{i,j} \hat{z}_j\}_{j < i}, \theta)\right), \quad (6)$$

357 where $\hat{\epsilon}_i$ is the transformed independent noise, $\log |J_i|$ is the Jacobian determinant, and NN denotes
 358 a neural network generating flow parameters. Assuming ϵ is factorized (e.g., $\mathcal{N}(0, I)$), the prior
 359 distribution is:

$$\log p(\hat{\mathbf{z}}; \theta) = \sum_i \left(\log p(\hat{\epsilon}_i) + \log |J_i| \right). \quad (7)$$

360 We implement an encoder $q_\phi(\hat{\mathbf{z}}|\mathbf{x}, \theta)$ that maps observed text embeddings \mathbf{x} into an approximate
 361 posterior over latent variables $\hat{\mathbf{z}}$. A decoder $p_\psi(\mathbf{x}|\mathbf{z}, \theta)$ reconstructs the observed embeddings from
 362 the true latent variables \mathbf{z} . The model is trained by maximizing the domain-conditioned Evidence
 363 Lower Bound (ELBO):

$$\mathcal{L}_{\text{ELBO}} = \mathbb{E}_{q_\phi(\hat{\mathbf{z}}|\mathbf{x}, \theta)} [\log p_\psi(\mathbf{x}|\hat{\mathbf{z}}, \theta)] - D_{\text{KL}}(q_\phi(\hat{\mathbf{z}}|\mathbf{x}, \theta) \parallel p(\mathbf{z}; \theta)), \quad (8)$$

364 where ϕ are encoder parameters, ψ are decoder parameters, and $p(\mathbf{z}; \theta)$ is the flow-based prior. To
 365 ensure the learned space is both causally structured and human-aligned, we add two regularizers:

$$\mathcal{L}_{\text{sparsity}} = \|\hat{W}\|_1, \quad \mathcal{L}_{\text{supervision}} = \frac{1}{K} \sum_{k=1}^K (\hat{c}_k - \tilde{c}_k)^2, \quad (9)$$

366 where $\hat{\mathbf{c}}$ are the estimated noisy concepts, $\tilde{\mathbf{c}}$ are LLM-inferred concepts, and K is the total latents.

378
379 **Table 3: Synthetic experiment results across different configurations.** We evaluate our method
380 against four baselines: β -VAE (reconstruction loss only), iVAE (independent VAE), Sun et al. (multi-
381 modal only), and Zhang et al. (multi-domain only). Results are reported as Pearson MCC and
382 Spearman MCC percentages. Our method consistently achieves higher MCC across most configura-
383 tions, demonstrating the effectiveness of combining multi-modal and multi-domain information.

Method	Linear				Nonlinear			
	Gaussian		Laplacian		Gaussian		Laplacian	
	Pearson	Spearman	Pearson	Spearman	Pearson	Spearman	Pearson	Spearman
Y Structure								
β -VAE	73.00 \pm 5.2	73.80 \pm 4.8	70.77 \pm 6.1	70.31 \pm 5.9	86.11 \pm 3.2	88.64 \pm 2.9	75.34 \pm 4.7	75.96 \pm 4.3
iVAE	51.63 \pm 8.4	51.12 \pm 7.9	39.33 \pm 9.2	37.00 \pm 8.7	53.02 \pm 6.8	51.41 \pm 6.5	12.25 \pm 3.1	13.43 \pm 2.8
Sun et al.	82.86 \pm 4.1	82.70 \pm 3.8	72.59 \pm 5.3	73.89 \pm 4.9	69.49 \pm 6.2	70.86 \pm 5.7	61.60 \pm 7.4	71.16 \pm 6.8
Zhang et al.	70.32 \pm 6.8	70.30 \pm 6.2	63.60 \pm 8.1	66.57 \pm 7.5	72.22 \pm 5.9	72.66 \pm 5.4	48.33 \pm 9.2	50.70 \pm 8.7
Ours	84.33\pm6.17	86.08\pm6.02	81.01\pm7.31	83.38\pm9.16	82.79\pm2.73	83.65\pm3.33	71.38 \pm 2.82	77.58 \pm 3.98
Chain Structure								
β -VAE	77.95 \pm 4.8	79.66 \pm 4.2	77.14 \pm 5.1	77.30 \pm 4.6	72.08 \pm 6.3	74.04 \pm 5.8	69.79 \pm 7.2	71.33 \pm 6.9
iVAE	46.99 \pm 7.2	45.83 \pm 6.8	46.47 \pm 8.1	49.04 \pm 7.6	50.87 \pm 5.9	49.32 \pm 5.4	8.87 \pm 2.4	12.44 \pm 2.1
Sun et al.	86.52 \pm 3.7	87.06 \pm 3.4	68.13 \pm 6.8	70.28 \pm 6.2	65.43 \pm 7.9	65.61 \pm 7.3	59.63 \pm 8.6	70.47 \pm 7.8
Zhang et al.	70.55 \pm 6.4	69.63 \pm 5.9	62.24 \pm 7.8	66.16 \pm 7.2	69.90 \pm 5.6	70.93 \pm 5.1	46.16 \pm 8.9	48.86 \pm 8.4
Ours	80.33\pm11.29	81.00\pm11.87	81.88\pm6.71	83.72\pm7.13	79.60\pm5.53	80.99\pm5.75	68.87 \pm 2.51	76.78 \pm 2.34

391 **Final objective.** The overall objective is:

$$\mathcal{L}_{\text{total}} = \mathcal{L}_{\text{ELBO}} + \lambda_1 \mathcal{L}_{\text{sparsity}} + \lambda_2 \mathcal{L}_{\text{supervision}}, \quad (10)$$

401 with λ_1, λ_2 balancing reconstruction, causal sparsity, and concept alignment. This design ensures that
402 the model (i) captures domain-dependent causal mechanisms via the flexible flow-based prior, (ii)
403 recovers human-interpretable dimensions by refining noisy LLM-derived concepts $\tilde{\mathbf{c}}$ into true latent
404 concepts \mathbf{c} , and (iii) retains additional capacity to uncover novel concepts beyond the predefined set.
405

406 4.4 SYNTHETIC EXPERIMENTS

408 **Baselines and Metrics.** We evaluate our method against four representative CRL baselines, each
409 emphasizing different modeling assumptions and trade-offs. β -VAE (Higgins et al., 2017) relies only
410 on reconstruction loss and encourages disentanglement but lacks explicit identifiability guarantees.
411 iVAE (Tomczak & Welling, 2018) introduces identifiable priors but does not exploit multi-domain or
412 multi-modal variation effectively. Sun et al. (Sun et al., 2025b) leverage multi-modal information
413 but assume a single domain setting, while Zhang et al. (Zhang et al., 2024) leverage multi-domain
414 variation in a general setting but are limited to a single modality. Our approach integrates both
415 multi-domain and multi-modal information simultaneously, directly addressing the limitations of
416 these baselines. For evaluation metrics, we adopt both Pearson MCC and Spearman MCC. Pear-
417 son measures linear alignment between learned and ground-truth causal factors, while Spearman
418 assesses monotonic rank-order consistency across values. Using both together provides a robust and
419 comprehensive view of causal discovery performance, with higher values indicating better recovery.
420

421 **Implementation Details.** We generate synthetic data with four latent variables under two canonical
422 causal structures: Y-structure and Chain-structure. Each domain contains 10,000 samples, with 20
423 heterogeneous simulated domains in total. The model architecture consists of an encoder-decoder
424 with two hidden layers (64 and 32 units), trained for 1,000 iterations using Adam with learning
425 rate 0.001 throughout. Key hyperparameters are: reconstruction weight 5.0, KL divergence weight
426 0.1, sparsity weight 0.01, and supervision weight 1.0. We test both Gaussian and Laplacian priors
427 extensively, with evaluation every 50 iterations, averaged across multiple random seeds for robustness.
428

429 **Results and Analysis.** Table 3 summarizes results across all configurations. First, iVAE consistently
430 performs the weakest, especially under nonlinear settings (e.g., Spearman MCC below 15% in
431 nonlinear Laplacian cases), showing that identifiable VAEs alone are insufficient without domain
432 or modality variation. Second, β -VAE performs reasonably well in linear settings (above 70%), but
433 performance degrades significantly under nonlinear distributions, reflecting its lack of identifiability.

432 Third, Sun et al. (multi-modal only) and Zhang
 433 et al. (multi-domain only) improve over β -VAE
 434 and iVAE in certain cases, but both struggle
 435 when only one type of variation is available. For
 436 instance, Sun et al. underperform in nonlinear
 437 chain structures, while Zhang et al. show sharp
 438 drops under nonlinear Laplacian settings. Fi-
 439 nally, our method consistently achieves the best
 440 or near-best MCC across all configurations, im-
 441 proving by 3–10 points over the strongest base-
 442 line. Notably, in challenging nonlinear Lapla-
 443 cian settings, our approach maintains high cor-
 444 relations (e.g., 77.58% Spearman in Y-structure
 445 and 76.78% in Chain-structure), while baselines
 446 deteriorate. These results confirm that leverag-
 447 ing both multi-domain and multi-modal infor-
 448 mation is critical for robust causal representation
 449 learning. Our method not only recovers known
 450 causal factors more faithfully but also demon-
 451 strates strong generalization across different domains.
 452

451 4.5 REAL-WORLD EXPERIMENT ON ICLR REBUTTAL DATASET

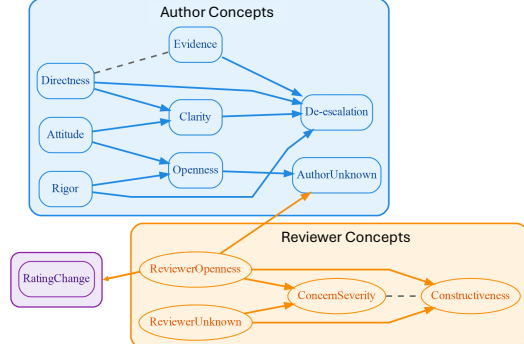
452 We apply our CRL framework to the ICLR rebuttal dataset to learn latent variables \mathbf{z} from review and
 453 rebuttal text, and then use causal discovery methods to recover the underlying causal graph (Fig. 4).
 454 Using 2393 labeled samples with 10 LLM-inferred concept labels, plus extensive unlabeled data,
 455 we train a MultiModalMarkovFlowVAE with separate encoders for reviewer (4 latent variables) and
 456 author (8 latent variables) modalities, each discovering one additional unknown concept. The learned
 457 causal graph (Fig. 5) shows that on the author side, *Clarity* plays a central role, influencing *Directness*,
 458 *Attitude*, and *De-escalation*, while *Openness* connects to *Rigor* and *Evidence*, highlighting how
 459 clear, transparent responses shape both tone and substance. On the reviewer side, *Review Quality*,
 460 *Reviewer Openness*, and *Concern Severity* form a tightly connected cluster, with *Reviewer Openness*
 461 directly driving *Rating Change*. Notably, two emergent latent concepts enrich this picture: the
 462 *Author_Unknown* node, connected to openness and influencing reviewer openness, likely reflects
 463 hidden aspects of persuasiveness or tone in author responses, while the *Reviewer_Unknown* node,
 464 linked with review quality and concern severity and directly affecting rating change, appears to
 465 capture latent reviewer dispositions such as strictness or flexibility. These results show that rebuttal
 466 effectiveness arises from both author strategies (clarity, evidence, rigor) and reviewer disposition,
 467 while latent factors further reveal subtle but impactful influences beyond predefined features.
 468
 469

470 5 DISCUSSIONS AND CONCLUSION

471 **Discussions.** A key limitation of our study is that the analysis is restricted to reviews from the ICLR
 472 2024 and 2025, which may limit the generalizability of the findings to other conferences or time
 473 periods. In addition, due to data availability constraints, we aggregate each paper’s reviews without
 474 accounting for the precise timestamps of individual revisions. As a result, our analysis do not capture
 475 the temporal dynamics of how rebuttals and reviewer ratings evolve over the review process.
 476

477 **Conclusions.** We presented a two-layer causal analysis of rebuttal effectiveness in ICLR 2024–2025
 478 submissions. At the structured layer, independence tests on metadata and LLM-inferred *concepts*
 479 revealed that clarity, directness, rigor, and evidence are most strongly linked to rating changes, while
 480 static paper descriptors play little role. At the unstructured layer, our causal representation learning
 481 framework refined noisy LLM-derived *concepts* and uncovered new latent dimensions, supported
 482 by identifiability guarantees. Together, these findings provide both theoretical insights into causal
 483 modeling of text and actionable guidance for the ML community: authors can focus on substantive,
 484 evidence-based rebuttals, while reviewers and chairs should remain aware of systematic influences on
 485 scoring. Our work thus contributes toward a more transparent, fair, and effective peer review process.

Figure 5: **Real-world experiment result.** This causal graph is learned by our proposed CRL method. Excepts the 10 given concepts, we also learn additional two concepts. See § 4.5 for details.



486 REFERENCES
487488 Kartik Ahuja, Divyat Mahajan, Yixin Wang, and Yoshua Bengio. Interventional causal representation
489 learning. In *International conference on machine learning*, pp. 372–407. PMLR, 2023.490 Bruce Alberts, Brooks Hanson, and Katrina L Kelner. Reviewing peer review, 2008.
491492 Jérôme Barrière, Fabrice Frank, Llonni Besançon, Alexander Samuel, Véronique Saada, Eric Billy,
493 Abraham Al-Ahmad, Barbara Seitz-Polski, and Jacques Robert. Scientific integrity requires
494 publishing rebuttals and retracting problematic papers. *Stem Cell Reviews and Reports*, 19(2):
495 568–572, 2023.
496497 Iz Beltagy, Kyle Lo, and Arman Cohan. Scibert: A pretrained language model for scientific text.
498 *arXiv preprint arXiv:1903.10676*, 2019.499 500 Yoshua Bengio, Tristan Deleu, Nasim Rahaman, Rosemary Ke, Sébastien Lachapelle, Olexa Bilaniuk,
501 Anirudh Goyal, and Christopher Pal. A meta-transfer objective for learning to disentangle causal
502 mechanisms. *arXiv preprint arXiv:1901.10912*, 2019.503 504 Michel Besserve, Naji Shajarisales, Bernhard Schölkopf, and Dominik Janzing. Group invariance
505 principles for causal generative models. In *International Conference on Artificial Intelligence and
Statistics*, pp. 557–565. PMLR, 2018.
506507 508 Stephen J Ceci and Douglas P Peters. Peer review: A study of reliability. *Change: The Magazine of
Higher Learning*, 14(6):44–48, 1982.509 510 Arman Cohan, Waleed Ammar, Madeleine Van Zuylen, and Field Cady. Structural scaffolds for
511 citation intent classification in scientific publications. *arXiv preprint arXiv:1904.01608*, 2019.512 513 Arman Cohan, Sergey Feldman, Iz Beltagy, Doug Downey, and Daniel S. Weld. Specter: Document-
514 level representation learning using citation-informed transformers, 2020. URL <https://arxiv.org/abs/2004.07180>.
515516 517 Michael Fromm, Evgeniy Faerman, Max Berrendorf, Siddharth Bhargava, Ruoxia Qi, Yao Zhang,
518 Lukas Dennert, Sophia Selle, Yang Mao, and Thomas Seidl. Argument mining driven analysis
519 of peer-reviews. In *Proceedings of the AAAI conference on artificial intelligence*, volume 35, pp.
4758–4766, 2021.520 521 Yang Gao, Steffen Eger, Ilia Kuznetsov, Iryna Gurevych, and Yusuke Miyao. Does my rebuttal
522 matter? insights from a major nlp conference. *arXiv preprint arXiv:1903.11367*, 2019.523 524 Arthur Gretton, Olivier Bousquet, Alex Smola, and Bernhard Schölkopf. Measuring statistical
525 dependence with hilbert-schmidt norms. In *International conference on algorithmic learning
theory*, pp. 63–77. Springer, 2005.
526527 528 Irina Higgins, Loic Matthey, Arka Pal, Christopher P Burgess, Xavier Glorot, Matthew M Botvinick,
529 Shakir Mohamed, and Alexander Lerchner. beta-vae: Learning basic visual concepts with a
constrained variational framework. *ICLR (Poster)*, 3, 2017.530 531 Junjie Huang, Win-bin Huang, Yi Bu, Qi Cao, Huawei Shen, and Xueqi Cheng. What makes a
532 successful rebuttal in computer science conferences?: A perspective on social interaction. *Journal
of Informetrics*, 17(3):101427, 2023.
533534 535 David Jurgens, Srijan Kumar, Raine Hoover, Dan McFarland, and Dan Jurafsky. Measuring the evolu-
536 tion of a scientific field through citation frames. *Transactions of the Association for Computational
Linguistics*, 6:391–406, 2018.
537538 539 David Klindt, Lukas Schott, Yash Sharma, Ivan Ustyuzhaninov, Wieland Brendel, Matthias Bethge,
and Dylan Paiton. Towards nonlinear disentanglement in natural data with temporal sparse coding.
arXiv preprint arXiv:2007.10930, 2020.

540 Sebastien Lachapelle, Pau Rodriguez, Yash Sharma, Katie E Everett, Rémi LE PRIOL, Alexandre
 541 Lacoste, and Simon Lacoste-Julien. Disentanglement via mechanism sparsity regularization:
 542 A new principle for nonlinear ICA. In Bernhard Schölkopf, Caroline Uhler, and Kun Zhang
 543 (eds.), *Proceedings of the First Conference on Causal Learning and Reasoning*, volume 177
 544 of *Proceedings of Machine Learning Research*, pp. 428–484. PMLR, 11–13 Apr 2022. URL
 545 <https://proceedings.mlr.press/v177/lachapelle22a.html>.

546 John Langford and Mark Guzdial. The arbitrariness of reviews, and advice for school administrators.
 547 *Communications of the ACM*, 58(4):12–13, 2015.

549 John Lawrence and Chris Reed. Argument mining: A survey. *Computational Linguistics*, 45(4):
 550 765–818, 2020.

552 Phillip Lippe, Sara Magliacane, Sindy Löwe, Yuki M Asano, Taco Cohen, and Stratis Gavves. Citris:
 553 Causal identifiability from temporal intervened sequences. In *International Conference on Machine
 554 Learning*, pp. 13557–13603. PMLR, 2022.

555 Ryan Liu, Steven Jecmen, Vincent Conitzer, Fei Fang, and Nihar B Shah. Testing for reviewer
 556 anchoring in peer review: A randomized controlled trial. *PloS one*, 19(11):e0301111, 2024.

558 Francesco Locatello, Stefan Bauer, Mario Lucic, Gunnar Raetsch, Sylvain Gelly, Bernhard Schölkopf,
 559 and Olivier Bachem. Challenging common assumptions in the unsupervised learning of disentan-
 560 gled representations. In *international conference on machine learning*, pp. 4114–4124. PMLR,
 561 2019.

562 Francesco Locatello, Ben Poole, Gunnar Rätsch, Bernhard Schölkopf, Olivier Bachem, and Michael
 563 Tschannen. Weakly-supervised disentanglement without compromises. In *International conference
 564 on machine learning*, pp. 6348–6359. PMLR, 2020.

566 Giambattista Parascandolo, Niki Kilbertus, Mateo Rojas-Carulla, and Bernhard Schölkopf. Learning
 567 independent causal mechanisms. In *International Conference on Machine Learning*, pp. 4036–4044.
 568 PMLR, 2018.

569 Sukannya Purkayastha, Zhuang Li, Anne Lauscher, Lizhen Qu, and Iryna Gurevych. Lazyreview a
 570 dataset for uncovering lazy thinking in nlp peer reviews. *arXiv preprint arXiv:2504.11042*, 2025.

572 Azzurra Ragone, Katsiaryna Mirylenka, Fabio Casati, and Maurizio Marchese. On peer review in
 573 computer science: Analysis of its effectiveness and suggestions for improvement. *Scientometrics*,
 574 97:317–356, 2013.

576 Goutham Rajendran, Simon Buchholz, Bryon Aragam, Bernhard Schölkopf, and Pradeep Ravikumar.
 577 From causal to concept-based representation learning. *Advances in Neural Information Processing
 578 Systems*, 37:101250–101296, 2024.

579 Tony Ross-Hellauer. What is open peer review? a systematic review. *F1000Research*, 6:588, 2017.

581 Bernhard Schölkopf, Francesco Locatello, Stefan Bauer, Nan Rosemary Ke, Nal Kalchbrenner,
 582 Anirudh Goyal, and Yoshua Bengio. Toward causal representation learning. *Proceedings of the
 583 IEEE*, 109(5):612–634, 2021.

585 Nihar B Shah, Behzad Tabibian, Krikamol Muandet, Isabelle Guyon, and Ulrike Von Luxburg.
 586 Design and analysis of the nips 2016 review process. *Journal of machine learning research*, 19
 587 (49):1–34, 2018.

588 Xinwei Shen, Furui Liu, Hanze Dong, Qing Lian, Zhitang Chen, and Tong Zhang. Weakly supervised
 589 disentangled generative causal representation learning. *Journal of Machine Learning Research*, 23
 590 (241):1–55, 2022.

592 Rui Shu, Yining Chen, Abhishek Kumar, Stefano Ermon, and Ben Poole. Weakly supervised
 593 disentanglement with guarantees. In *International Conference on Learning Representations*. ICLR,
 2020.

594 Ivan Stelmakh, Nihar B Shah, Aarti Singh, and Hal Daumé III. Prior and prejudice: The novice
 595 reviewers' bias against resubmissions in conference peer review. *Proceedings of the ACM on*
 596 *Human-Computer Interaction*, 5(CSCW1):1–17, 2021.

597

598 Eric V Strobl, Kun Zhang, and Shyam Visweswaran. Approximate kernel-based conditional indepen-
 599 dence tests for fast non-parametric causal discovery. *Journal of Causal Inference*, 7(1):20180017,
 600 2019.

601 Hao Sun, Yunyi Shen, and Mihaela van der Schaar. Openreview should be protected and leveraged as a
 602 community asset for research in the era of large language models. *arXiv preprint arXiv:2505.21537*,
 603 2025a.

604

605 Yuewen Sun, Lingjing Kong, Guangyi Chen, Loka Li, Gongxu Luo, Zijian Li, Yixuan Zhang, Yujia
 606 Zheng, Mengyue Yang, Petar Stojanov, et al. Causal representation learning from multi-modal
 607 biomedical observations. *ArXiv*, pp. arXiv–2411, 2025b.

608 Ronald J Tallarida, Rodney B Murray, Ronald J Tallarida, and Rodney B Murray. Chi-square test.
 609 *Manual of pharmacologic calculations: with computer programs*, pp. 140–142, 1987.

610

611 Chenhao Tan, Vlad Niculae, Cristian Danescu-Niculescu-Mizil, and Lillian Lee. Winning arguments:
 612 Interaction dynamics and persuasion strategies in good-faith online discussions. In *Proceedings of*
 613 *the 25th international conference on world wide web*, pp. 613–624, 2016.

614 Jonathan P Tennant. The state of the art in peer review. *FEMS Microbiology letters*, 365(19):fnv204,
 615 2018.

616

617 Jonathan P Tennant and Tony Ross-Hellauer. The limitations to our understanding of peer review.
 618 *Research integrity and peer review*, 5(1):6, 2020.

619 Jakub Tomczak and Max Welling. Vae with a vampprior. In *International conference on artificial*
 620 *intelligence and statistics*, pp. 1214–1223. PMLR, 2018.

621

622 Andrew Tomkins, Min Zhang, and William D Heavlin. Reviewer bias in single-versus double-blind
 623 peer review. *Proceedings of the National Academy of Sciences*, 114(48):12708–12713, 2017.

624

625 David Tran, Alex Valtchanov, Keshav Ganapathy, Raymond Feng, Eric Slud, Micah Goldblum,
 626 and Tom Goldstein. An open review of openreview: A critical analysis of the machine learning
 627 conference review process. *arXiv preprint arXiv:2010.05137*, 2020.

628

629 Ioannis Tsamardinos, Laura E Brown, and Constantin F Aliferis. The max-min hill-climbing bayesian
 630 network structure learning algorithm. *Machine learning*, 65:31–78, 2006.

631

632 David Wadden, Kyle Lo, Lucy Lu Wang, Arman Cohan, Iz Beltagy, and Hannaneh Hajishirzi.
 633 Multivers: Improving scientific claim verification with weak supervision and full-document
 634 context. In *Findings of the Association for Computational Linguistics: NAACL 2022*, pp. 61–76,
 2022.

635

636 Gang Wang, Qi Peng, Yanfeng Zhang, and Mingyang Zhang. What have we learned from openreview?
 637 *World Wide Web*, 26(2):683–708, 2023a.

638

639 Jianyou Andre Wang, Kaicheng Wang, Xiaoyue Wang, Prudhviraj Naidu, Leon Bergen, and Ra-
 640 mamohan Paturi. Scientific document retrieval using multi-level aspect-based queries. *Advances*
 641 *in Neural Information Processing Systems*, 36:38404–38419, 2023b.

642

643 Antoine Wehenkel and Gilles Louppe. Unconstrained monotonic neural networks. *Advances in*
 644 *neural information processing systems*, 32, 2019.

645

646 Dietmar Wolfram, Peiling Wang, Adam Hembree, and Hyoungjoo Park. Open peer review: promoting
 647 transparency in open science. *Scientometrics*, 125(2):1033–1051, 2020.

648

649 Po-Cheng Wu, An-Zi Yen, Hen-Hsen Huang, and Hsin-Hsi Chen. Incorporating peer reviews
 650 and rebuttal counter-arguments for meta-review generation. In *Proceedings of the 31st ACM*
 651 *International Conference on Information & Knowledge Management*, pp. 2189–2198, 2022.

648 Danru Xu, Dingling Yao, Sébastien Lachapelle, Perouz Taslakian, Julius von Kügelgen, Francesco
649 Locatello, and Sara Magliacane. A sparsity principle for partially observable causal representation
650 learning. *arXiv preprint arXiv:2403.08335*, 2024.

651

652 Jing Yang. Paper copilot: The artificial intelligence and machine learning community should adopt a
653 more transparent and regulated peer review process. *arXiv e-prints*, pp. arXiv–2502, 2025.

654

655 Dingling Yao, Danru Xu, Sébastien Lachapelle, Sara Magliacane, Perouz Taslakian, Georg Martius,
656 Julius von Kügelgen, and Francesco Locatello. Multi-view causal representation learning with
657 partial observability. *arXiv preprint arXiv:2311.04056*, 2023.

658

659 Dingling Yao, Dario Rancati, Riccardo Cadei, Marco Fumero, and Francesco Locatello. Unifying
660 causal representation learning with the invariance principle. *arXiv preprint arXiv:2409.02772*,
661 2024.

662

663 Kun Zhang, Jonas Peters, Dominik Janzing, and Bernhard Schölkopf. Kernel-based conditional
664 independence test and application in causal discovery. *arXiv preprint arXiv:1202.3775*, 2012.

665

666 Kun Zhang, Shaoan Xie, Ignavier Ng, and Yujia Zheng. Causal representation learning from multiple
667 distributions: A general setting. *arXiv preprint arXiv:2402.05052*, 2024.

668

669

670

671

672

673

674

675

676

677

678

679

680

681

682

683

684

685

686

687

688

689

690

691

692

693

694

695

696

697

698

699

700

701

702 *Appendix for*
703704 **“How Effective is Your Rebuttal? Identifying Causal Models from the**
705 **OpenReview System”**706 Table of Contents:
707

710 A1 Ethics Statement	14
711	
712 A2 The use of large language models (LLMs)	14
713	
714 A3 Details about Related Work	15
715	
716 A3.1 Peer Review Analysis	15
717	
718 A3.2 Causal Representation Learning	15
719	
720 A3.3 Natural Language Processing for Scientific Text	15
721 A4 Details about the Dataset and Analysis	15
722	
723 A4.1 Explanation of Concept Features in Tab.2	15
724	
725 A4.2 Explanation of Variables in Fig.1	16
726	
727 A4.3 Dataset Analysis	16
728 A5 Learning Human-aligned Causal Representations	17
729	
730 A5.1 Basic Concept	17
731	
732 A5.2 Identifiability of Causal Models: Theorem and Proof	18

733
734 **A1 ETHICS STATEMENT**

735 All datasets used in this work are restricted to non-commercial, academic research purposes. We
736 obtained the necessary permissions from the respective platforms. A summary of the applicable
737 terms-of-use is as follows:

- 738 • **ICLR** – Submissions and reviews are hosted on OpenReview under an open-access license
739 (CC BY 4.0), which explicitly permits reuse for research purposes.
- 740 • **PaperCopilot** – According to its Terms of Use, no part of the Site’s content may be copied,
741 reproduced, distributed, or otherwise exploited for commercial purposes without express
742 prior written permission. We obtained such permission and consent directly from the website
743 to enable non-commercial and academic research use.

744 **A2 THE USE OF LARGE LANGUAGE MODELS (LLMs)**

745 We employ large language models (LLMs) to infer author- and reviewer-related concepts from textual
746 inputs in our dataset. To ensure robustness and model fit, we conducted a comparative evaluation
747 across candidate LLMs and selected the most suitable model for this task (Tab. 2). In line with
748 community guidance on LLM usage, we explicitly disclose this use and retain full responsibility for
749 the accuracy and integrity of all LLM-derived outputs. For transparency and reproducibility, we also
750 provide the exact inference prompt used in our pipeline (App. 1), enabling independent verification
751 and replication of our procedure.

756 **A3 DETAILS ABOUT RELATED WORK**
757758 **A3.1 PEER REVIEW ANALYSIS**
759

760 Peer review in scientific publishing has been widely studied, with work addressing bias (Tomkins
761 et al., 2017), consistency (Langford & Guzdial, 2015), and predictive validity (Ragone et al., 2013).
762 The transparency of the OpenReview platform has further enabled analyses of reviewer behavior and
763 decision-making (Stelmakh et al., 2021; Gao et al., 2019). Recent studies provide complementary
764 perspectives. (Liu et al., 2024) conducted a randomized controlled trial and found that reviewers are
765 not strongly anchored to their initial scores, showing a willingness to revise after rebuttals, though the
766 drivers of such changes remain unclear. The LazyReview dataset (Purkayastha et al., 2025) addresses
767 a different challenge by identifying low-effort or vague reviews, offering tools to improve review
768 quality. By contrast, the effectiveness of rebuttals themselves has received relatively limited attention.
769 (Shah et al., 2018) showed that rebuttals lead to score changes in about 25% of reviews, while (Gao
770 et al., 2019) explored correlates of successful rebuttals without establishing causality. Our work
771 extends these efforts by explicitly modeling the causal mechanisms underlying rebuttal effectiveness.
772

773 **A3.2 CAUSAL REPRESENTATION LEARNING**
774

775 Causal representation learning (CRL) seeks to uncover latent causal factors from high-dimensional
776 data (Schölkopf et al., 2021; Parascandolo et al., 2018), enabling reasoning about interventions and
777 counterfactuals. Recent work has shown that CRL can learn disentangled representations capturing
778 causal mechanisms (Lachapelle et al., 2022; Lippe et al., 2022), making it particularly useful in
779 domains where causal factors are latent or noisy, such as peer review. Unsupervised CRL methods
780 face identifiability challenges (Locatello et al., 2019), which researchers have attempted to address
781 using temporal structure (Klindt et al., 2020), sparsity assumptions (Bengio et al., 2019), or group-
782 theoretic frameworks (Besserve et al., 2018). However, such assumptions often fail in real-world
783 settings. To overcome this, weak supervision and multi-environment data have been proposed to
784 improve identifiability (Locatello et al., 2020; Shu et al., 2020). Building on weakly supervised
785 approaches (Shen et al., 2022) and concept-based representation learning (Rajendran et al., 2024),
786 our work adapts these ideas to model rebuttal effectiveness.

787 **A3.3 NATURAL LANGUAGE PROCESSING FOR SCIENTIFIC TEXT**
788

789 Analyzing rebuttals requires handling complex scientific text. Advances in natural language processing
790 have enabled richer analysis of scientific documents (Beltagy et al., 2019; Cohan et al., 2020),
791 supporting tasks such as classification, summarization, citation intent detection (Cohan et al., 2019;
792 Jurgens et al., 2018), document retrieval (Wang et al., 2023b), and fact-checking (Wadden et al.,
793 2022). While less explored, rebuttals have been studied through argument mining (Lawrence & Reed,
794 2020; Fromm et al., 2021) and persuasive language (Tan et al., 2016), reflecting their persuasive
795 nature in influencing reviewer opinions.

796 Our work connects these directions by applying causal representation learning to study rebuttal
797 effectiveness in scientific peer review, focusing on the OpenReview system in machine learning
798 conferences.

799 **A4 DETAILS ABOUT THE DATASET AND ANALYSIS**
800801 **A4.1 EXPLANATION OF CONCEPT FEATURES IN TAB.2**
802

803 We consider ten variables capturing key aspects of rebuttals and reviews. *Clarity* (*CL*) reflects how
804 clearly the rebuttal communicates its arguments, while *Directness* (*DI*) measures the extent to which it
805 addresses reviewer concerns explicitly. *Attitude* (*AT*) captures the tone of the rebuttal, distinguishing
806 professional and respectful responses from defensive ones. *Authors Openness* (*AO*) denotes the
807 willingness of authors to acknowledge limitations or alternative perspectives. *Evidence* (*EV*) refers to
808 the use of data, experiments, or citations to support claims, and *Rigor* (*RI*) evaluates the technical
809 soundness and thoroughness of rebuttal arguments. *De-Escalation* (*DE*) reflects the ability to resolve
810 misunderstandings and reduce conflict during the exchange. On the reviewer side, *Review Quality*

(*RQ*) measures the specificity and constructiveness of feedback, *Reviewer Openness* (*RO*) captures the willingness of reviewers to revise their evaluation in light of rebuttals, and *Concern Severity* (*CS*) indicates the seriousness of the issues raised in the review.

A4.2 EXPLANATION OF VARIABLES IN FIG.1

We further include metadata and reviewer-provided variables. *Title Length* and *Abstract Length* measure the verbosity of the submission’s title and abstract, respectively, while *Num Authors* captures the number of contributing authors. *Status* indicates the acceptance outcome (e.g., oral, poster, reject), and *Primary Area* records the main research domain of the paper. *Num Interactions* reflects the extent of back-and-forth exchanges between authors and reviewers. Reviewer scores are also considered: *Soundness* assesses methodological correctness, *Presentation* evaluates clarity of exposition, and *Contribution* reflects novelty and significance. Finally, *aoor_rating_diff* measures the average of other reviews’s rating differences or changes for one reviewer; we define this variable in order to see how one reviewer can be influenced by other reviewers.

A4.3 DATASET ANALYSIS

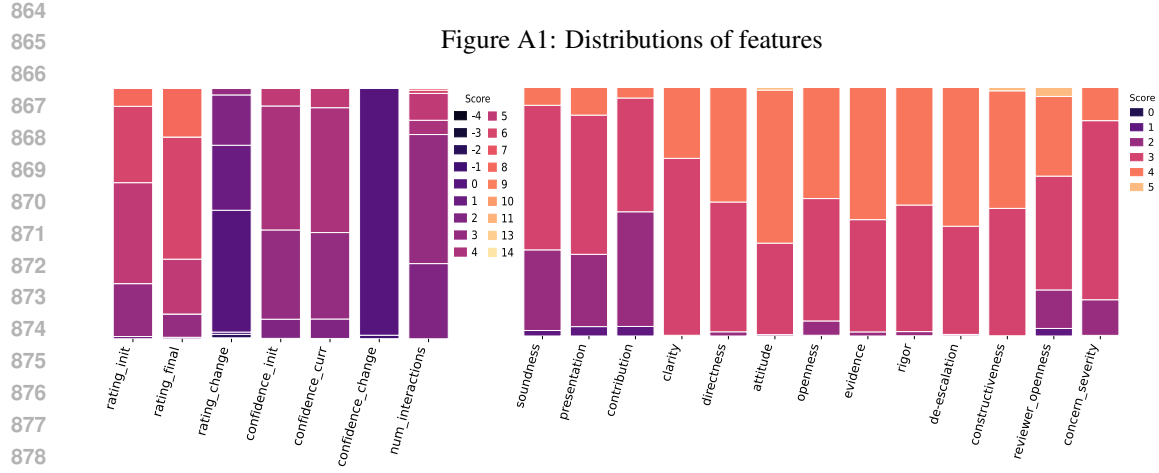
For fine-grained analysis, we annotate a 10% random sample of the dataset with interpretable labels capturing both rebuttal quality and reviewer behavior. Rebuttal-related dimensions include *Clarity*, *Directness in Addressing Reviewer Concerns*, *Positive Attitude*, *Willingness to Acknowledge Limitations*, *Strength of Evidence*, *Technical Convincingness and Rigor*, and *Handling of Misunderstandings and De-escalation*, while reviewer-related dimensions include *Review Specificity and Constructiveness*, *Open-mindedness*, and *Severity of Concerns*. All labels are rated on a 5-point ordinal scale, with detailed guidelines provided in the annotation prompt (Appendix).

To construct the annotated subset, we manually labeled 20 review–rebuttal threads and used them to benchmark 10 LLMs. We then computed the L-2 distance between model predictions and human labels across dimensions. As shown in Table 2, DeepSeek-R1 achieved the closest alignment to human annotations and was chosen to label the full 10% set.

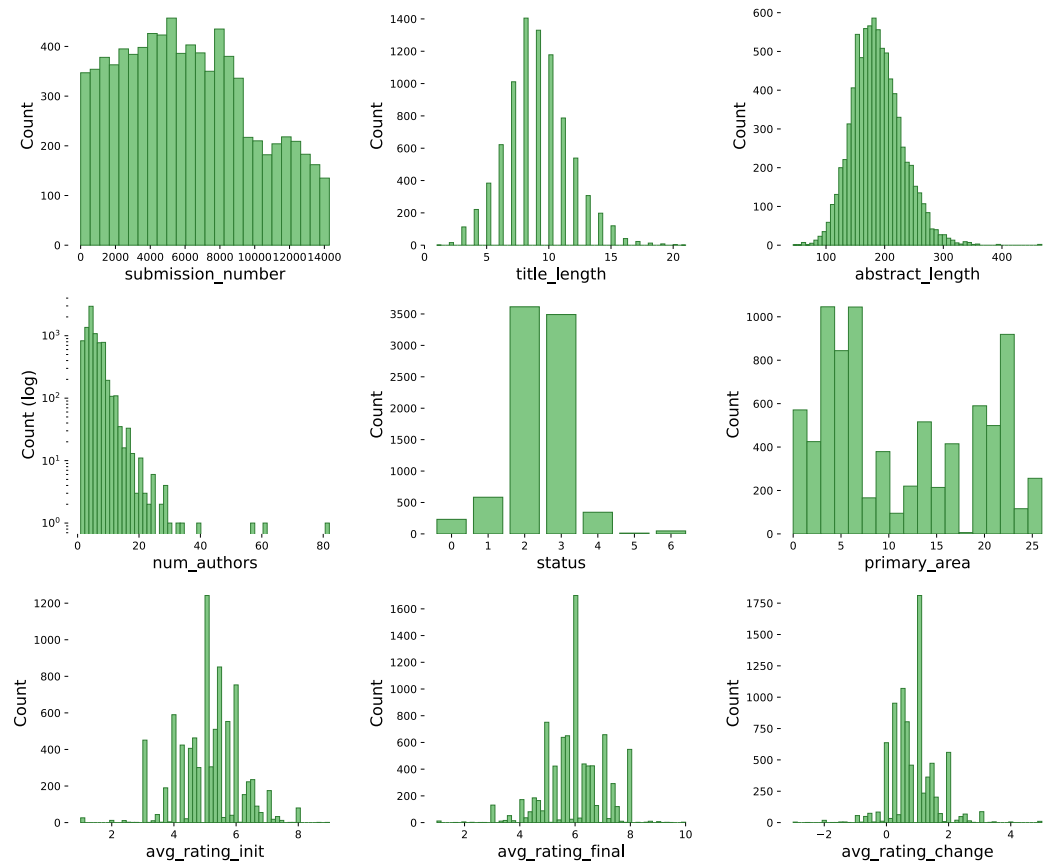
In addition to the annotated labels, we extract further labels from OpenReview, including metadata such as *Title Length*, *Abstract Length*, *Number of Authors*, *Status*, *Primary Area*, and *Number of Reviewer-Author(s) Interactions*, as well as reviewer-provided scores *Soundness*, *Presentation*, *Contribution*, *Initial Rating*, *Final Rating*, *Initial Confidence*, and *Final Confidence*. Using this subset, we conduct pairwise independence tests with Kernel-based Conditional Independence (KCI), Randomized Conditional Independence (RCSI), Hilbert-Schmidt Independence Criterion (HSIC), Chi-squared, and G-squared tests. Detailed results for each method are given in the Appendix A5.2. Figure 1 summarizes the findings, where each cell shows how many of the five tests failed to reject the null hypothesis.

The aggregated results in Figure 1 reveal several patterns. *Rating Difference* shows strong dependence with *Openness*, *Evidence*, and *Rigor*, suggesting that reviewers who initially gave low scores are more likely to revise them when faced with open, well-supported, and rigorous rebuttals. *Number of Interaction* is also dependent on *Rating Difference*, reflecting the role of back-and-forth communication in driving score changes. By contrast, *Clarity*, *Directness*, and *Attitude* show no dependence with *Rating Difference*, likely due to their skewed distribution (most rebuttals score highly, leaving little variability) or the selection bias of top-tier conference submissions, where both papers and reviews tend to be of consistently high quality. Interestingly, *Clarity* and *Attitude* do show dependence with *Initial Rating* and *Final Rating*, but not with *Rating Difference*, implying that they shape the overall impression of a paper without directly influencing score updates.

We also find that *Reviewer Openness* and *Severity of Concerns* are strongly associated with *Rating Difference*, indicating that large score changes occur when open-minded reviewers engage with rebuttals addressing serious issues. In contrast, metadata features such as *Title Length*, *Abstract Length*, *Number of Authors*, and *Primary Area* show no dependence on *Rating Difference*, suggesting they play only a minor role compared to content-based signals. The dependence of *Status* on *Initial Rating*, *Final Rating*, and *Rating Difference* is expected, as decisions (e.g., oral, poster) follow review scores. Finally, *Confidence* scores appear largely independent of other features, suggesting they are influenced by external factors.



880 Figure A2: Paper-level metadata feature distributions; see Appendix A1 for primary area details.



A5 LEARNING HUMAN-ALIGNED CAUSAL REPRESENTATIONS

A5.1 BASIC CONCEPT

To connect abstract latent variables with human-understandable criteria, we model review subscores (e.g., soundness, clarity, novelty) as *concepts*. Formally, each concept is defined as a linear projection $A : \mathbb{R}^{d_z} \rightarrow \mathbb{R}^{d_C}$ of the latent rebuttal representation \mathbf{z} , with a valuation $b \in \mathbb{R}^{d_C}$ corresponding to the reviewer's assigned subscore (e.g., clarity = 4). Thus, rebuttals with the same subscore form

918 a concept-conditional set in latent space. This formulation anchors the learned representations to
 919 interpretable axes aligned with reviewer evaluations.
 920

921 A5.2 IDENTIFIABILITY OF CAUSAL MODELS: THEOREM AND PROOF

923 **Theorem 1. (Identifiability of Review Concepts)** Suppose we match the observations \mathbf{x}_m across
 924 modalities (authors and reviewers), and the following conditions hold in the data-generating process:

925 *i (Information Preservation):* The functions g_1 and g_2 are differentiable and invertible.

927 *ii (Primary Area Diversity):* All entries of $v^\top B$ are non-zero, where $B_{i,j} = \frac{b_k^e}{\sigma^2}$ denotes the
 928 area-concept matrix.

929 *iii (Thought Reflection):* The latent components in \mathbf{z}_1 are causal parents of \mathbf{z}_2 , but not vice versa.

930 *iv (Distinctive Concept Alignment):* There exists a set of linearly independent aligning vectors
 931 $\mathcal{C} = \{a_1, \dots, a_n\}$ such that, for each concept C^e , the rows of the aligning matrix A^e lie in
 932 \mathcal{C} , i.e., $(A^e)^\top e_i \in \mathcal{C}$. Let S^e denote the indices of the subset of \mathcal{C} that appear as rows of A^e .
 933 Every aligning vector in \mathcal{C} appears in at least one area e (where an area corresponds to a
 934 concept-conditional distribution), that is,

$$\bigcup_e S^e = [n].$$

935 Then the review concepts are identifiable as in Definition 1.

936 **Discussion of Assumptions** Assumption i requires that the latent space is recoverable from the
 937 observed data. Assumption ii further requires the presence of latent distribution shifts in the review
 938 concepts across different primary areas, ensuring variability in the underlying structure. Assump-
 939 tion iii reflects the natural process in which authors first read the reviews, then engage in reflection,
 940 and finally provide rebuttals. Finally, Assumption iv ensures that all concepts can be decomposed
 941 into a finite set of atomic components that remain distinct across primary areas, which is essential for
 942 separating and identifying them.

943 **Proof Sketch** We first recover the latent space from the reviews and author responses by applying
 944 the inverse generating functions together with the fixed causal direction between the author and review
 945 modules. The presence of latent distribution shifts in the review concepts across different primary
 946 areas then provides additional variation, which allows us to identify each concept by comparing the
 947 concept spaces across environments. In this way, the atomic concepts can be causally inferred.

948 **Overview.** We prove that the review-side concepts are identifiable in the OpenReview system under
 949 Assumptions i–iv. Authors and reviewers provide two observed modalities $(\mathbf{x}_1, \mathbf{x}_2)$ generated from
 950 latent variables $(\mathbf{z}_1, \mathbf{z}_2)$. True human-aligned concepts are linear functionals of the latents, $\mathbf{c} = A\mathbf{z}$,
 951 while the LLM only yields noisy surrogates $\tilde{\mathbf{c}}$ defined by $\tilde{c}_{m,i} = c_{m,i} + \eta_{m,i}$ with Gaussian noise
 952 $\eta_{m,i}$. Our argument follows five steps: first we pass to a canonical latent parameterization; next we
 953 obtain a key observable identity; then we identify the concepts in different primary areas; after that,
 954 we recover primary-area valuations; finally, we remove residual symmetries to obtain uniqueness
 955 of the concept coordinates (up to permutation and scaling), matching Definition 1. Throughout this
 956 proof, “environments” are *primary areas* of OpenReview.

957 Assumption i states that both observation maps g_1, g_2 are differentiable and invertible, hence

$$(\mathbf{z}_1, \mathbf{z}_2) = (g_1^{-1}(\mathbf{x}_1), g_2^{-1}(\mathbf{x}_2)).$$

958 Assumption iii fixes the causal direction: reviewer latents \mathbf{z}_2 are parents of response latents \mathbf{z}_1
 959 (reviews influence responses), which rules out label-swap artifacts between the two modalities.

960 Let the atomic concept directions be the rows of the alignment map A , denoted $\mathcal{C} = \{a_1, \dots, a_n\}$.
 961 For each primary area e , let A^e collect the active rows and b^e be the associated valuations. Introduce
 962 the primary-area-concept incidence matrix $M \in \mathbb{R}^{m \times n}$ and the primary-area-valuation matrix
 963 $B \in \mathbb{R}^{m \times n}$ by

$$M_{ei} = \begin{cases} \sigma_i^{-2}, & \text{if } a_i \text{ is a row of } A^e, \\ 0, & \text{otherwise,} \end{cases} \quad B_{ei} = \begin{cases} \sigma_i^{-2} b_k^e, & \text{if the } k\text{-th row of } A^e \text{ equals } a_i, \\ 0, & \text{otherwise.} \end{cases} \quad (11)$$

Writing q_{σ^2} for a centered Gaussian with variance σ^2 , the primary-area densities satisfy

$$\ln p(\mathbf{z}) - \ln p_e(\mathbf{z}) = \sum_{i=1}^n \left(\frac{1}{2} M_{ei} \langle a_i, \mathbf{z} \rangle^2 - B_{ei} \langle a_i, \mathbf{z} \rangle \right) + c_e, \quad (12)$$

for constants c_e .

To place the model in standard coordinates, pick an invertible $T \in \mathbb{R}^{d_z \times d_z}$ with $T^{-\top} a_i = e_i$ for $1 \leq i \leq n$, a shift $\lambda \in \mathbb{R}^{d_z}$ with $\lambda_i = 0$ for $i > n$, and a diagonal matrix Σ with $\Sigma_{ii} = \sigma_i$ for $i \leq n$ and $\Sigma_{ii} = 1$ otherwise. Define the affine reparameterization

$$L(z) = \Sigma^{-1} T z - \lambda. \quad (13)$$

Push the model through L :

$$z = L(\mathbf{z}), \quad g_m \leftarrow g_m \circ L^{-1}, \quad A^e \leftarrow A^e T^{-1}, \quad p(z) = p(L^{-1} z) |\det T^{-1}|. \quad (14)$$

If the k -th row of A^e equals a_i , update

$$b_k^e \leftarrow b_k^e / \sigma_i - \lambda_i. \quad (15)$$

In this standard form all nonzero entries of M are 1, and

$$M = M \text{Diag}(\sigma_1^2, \dots, \sigma_n^2), \quad B = B \text{Diag}(\sigma_1^{-1}, \dots, \sigma_n^{-1}) - M \text{Diag}(\lambda_1, \dots, \lambda_n). \quad (16)$$

The observed distributions are unchanged (only the Jacobian modifies densities), so both parameterizations generate the same $(\mathbf{x}_1, \mathbf{x}_2)$. Choose λ so each row of B has mean zero across primary areas, and flip any coordinate z_i so that the first nonzero entry in column i of B is positive. Assumption ii is stable under this normalization: $v^\top M = 0$ and $v^\top B \neq 0$ before the transformation implies the same after diagonal rescaling and centering. We henceforth work in this standard form.

Define the latent log-density contrasts

$$g_e(z) := \ln p_0(z) - \ln p_e(z) = \sum_{i=1}^n \left(\frac{1}{2} M_{ei} z_i^2 - B_{ei} z_i \right) - c'_e, \quad (17)$$

where p_0 is the observational mixture over primary areas. On the observation side, set

$$G_e(x) := \ln p_X^0(x) - \ln p_X^e(x). \quad (18)$$

Because g_m are diffeomorphisms on the data manifold, Jacobians cancel in differences and

$$g_e(z) = G_e(g(z)) = G_e(x). \quad (19)$$

Even when g maps into a submanifold (if $d_z \neq d_x$), local charts yield the same difference; hence G_e is identifiable from data and so are geometric features of argmin sets of $\sum_{e \in T} g_e$.

Let $S^e = \{i \in [n] : a_i \text{ is a row of } A^e\}$ be the active atoms in area e . For $T \subset [m]$, write $S^T = \bigcup_{e \in T} S^e$ and consider

$$I_T := \arg \min_z \sum_{e \in T} g_e(z). \quad (20)$$

Since g_e are convex quadratics that separate across coordinates, there exist univariate convex functions h_i^T with

$$\sum_{e \in T} g_e(z) = \sum_{i=1}^n h_i^T(z_i), \quad h_i^T(z_i) = \begin{cases} \text{strictly convex with unique minimizer } z_i^T, & i \in S^T, \\ 0, & i \notin S^T. \end{cases} \quad (21)$$

Therefore

$$I_T = \{z \in \mathbb{R}^{d_z} : z_i = z_i^T \text{ for all } i \in S^T\}, \quad \dim(I_T) = d_z - |S^T|. \quad (22)$$

Using $g_e(z) = G_e(g(z))$,

$$g(I_T) = \arg \min_x \sum_{e \in T} G_e(x), \quad (23)$$

1026 and $\dim g(I_T) = \dim(I_T)$ because g is a diffeomorphism on the data manifold. Hence $|S^T|$ is
 1027 identifiable for every $T \subset [m]$. In particular, $n = |S^{[m]}|$ (each atom appears in at least one primary
 1028 area by Assumption iv).

1029 Knowing all $|S^T|$ recovers M up to a permutation of columns (relabeling concepts). An induction on
 1030 m is standard: when $m = 1$, $|S^{\{1\}}|$ counts active atoms in the first area; for the step $m \rightarrow m+1$, the
 1031 values $|S^{T \cup \{m+1\}}|$ across $T \subset [m]$ reveal which columns satisfy $M_{m+1,i} = 1$, and the differences
 1032 $|S^T| - |S^{T \cup \{m+1\}}|$ identify the columns with $M_{m+1,i} = 0$. Thus M is identified up to column
 1033 permutation.

1034 Fix an atom i and define

$$I_{T_i} = \{e \in [m] : M_{ei} = 0\}. \quad (24)$$

1035 By Assumption iv (distinctive alignment), for every $i' \neq i$ there exists an area that filters i' , hence
 1036 $S^{T_i} = [n] \setminus \{i\}$. Consequently,

$$I_{T_i} = \{z \in \mathbb{R}^{d_z} : z_{i'} = z_{i'}^{T_i} \text{ for all } i' \neq i\}, \quad (25)$$

1037 so only z_i varies on I_{T_i} . For any area e with $i \in S^e$ (so $M_{ei} = 1$ in standard form),

$$g_e(z) = c_e^{T_i} + \frac{1}{2}z_i^2 - B_{ei}z_i \quad \text{on } I_{T_i}. \quad (26)$$

1038 If $e_1 \neq e_2$ both contain i , define the slice where g_{e_1} is minimized:

$$I_{T_i}^{e_1} = \arg \min_{z \in I_{T_i}} g_{e_1}(z) = \{z \in I_{T_i} : z_i = B_{e_1 i}\}. \quad (27)$$

1039 Evaluating g_{e_2} on $I_{T_i}^{e_1}$ and subtracting its minimum over I_{T_i} gives

$$\min_{z \in I_{T_i}^{e_1}} g_{e_2}(z) - \min_{z \in I_{T_i}} g_{e_2}(z) = \frac{(B_{e_1 i} - B_{e_2 i})^2}{2}. \quad (28)$$

1040 The left-hand side is observable since $g(I_{T_i}) = \arg \min_x \sum_{e \in T_i} G_e(x)$ is identifiable and we can
 1041 minimize G_{e_2} over $g(I_{T_i})$. Hence $|B_{e_1 i} - B_{e_2 i}|$ is identified for all pairs with i active. Choose the
 1042 pair with maximal separation to bracket all B_{ei} for $i \in S^e$; the zero-mean row constraint from Step 1
 1043 fixes the additive constant and the “first nonzero positive” convention fixes the sign. Repeating over i
 1044 identifies B (up to the same column permutation as M).

1045 Consider two standard-form representations (z, g, p) and $(\tilde{z}, \tilde{g}, \tilde{p})$ that share (M, B) . Let $\varphi = \tilde{g}^{-1} \circ g$.
 1046 Decompose $z = (z_c, z_o)$ with $z_c \in \mathbb{R}^n$ the concept coordinates and $z_o \in \mathbb{R}^{d_z - n}$ the complement; fix
 1047 z_o and set $\iota_o(z_c) = (z_c, z_o)$ and $\varphi_o(z_c) = \pi_c(\varphi(\iota_o(z_c)))$, where π_c projects to the first n coordinates.
 1048 Since g_e depends only on (M, B) in both models,

$$g(\iota_o(z_c)) = G(g(\iota_o(z_c))) = G(\tilde{g}(\varphi(\iota_o(z_c)))) = g(\varphi_o(z_c)), \quad (29)$$

1049 with $g = (g_e)_{e=1}^m$ and $G = (G_e)_{e=1}^m$. Differentiating,

$$Dg_e(z) = M_{ei}z_i - B_{ei}, \quad Dg(z) = M \text{Diag}(z_1, \dots, z_n) - B, \quad (30)$$

1050 so for $z = \iota_o(z_c)$ and $\tilde{z} = \iota_o(\varphi_o(z_c))$,

$$M \text{Diag}(z_1, \dots, z_n) - B = (M \text{Diag}(\tilde{z}_1, \dots, \tilde{z}_n) - B) D\varphi_o(z_c). \quad (31)$$

1051 Let M^+ be a left pseudoinverse of M (rank n holds by coverage and linear independence), and
 1052 choose v from Assumption ii with $v^\top M = 0$ and $v^\top B \neq 0$. Stacking yields

$$\tilde{M}^+ = \begin{pmatrix} M^+ \\ v^\top \end{pmatrix} \in \mathbb{R}^{(n+1) \times m}, \quad (32)$$

1053 and multiplying,

$$\begin{pmatrix} z_1 & 0 & \cdots & 0 \\ \ddots & \ddots & & \vdots \\ 0 & \cdots & z_n & 0 \\ 0 & \cdots & 0 & 0 \end{pmatrix} - \tilde{M}^+ B = \left(\begin{pmatrix} \tilde{z}_1 & 0 & \cdots & 0 \\ \ddots & \ddots & \ddots & \vdots \\ 0 & \cdots & \tilde{z}_n & 0 \\ 0 & \cdots & 0 & 0 \end{pmatrix} - \tilde{M}^+ B \right) D\varphi_o(z_c). \quad (33)$$

1080

1081

Table A1: Primary areas and counts

ID	Primary Area	Counts
0	General machine learning (i.e., none of the above)	295
1	Transfer learning, meta learning, and lifelong learning	274
2	Datasets and benchmarks	425
3	Representation learning for computer vision, audio, language, and other modalities	360
4	Unsupervised, self-supervised, semi-supervised, and supervised representation learning	686
5	Generative models	844
6	Reinforcement learning	637
7	Applications to physical sciences (physics, chemistry, biology, etc.)	408
8	Applications to neuroscience & cognitive science	166
9	Learning theory	284
10	Causal reasoning	96
11	Neurosymbolic & hybrid AI systems (physics-informed, logic & formal reasoning, etc.)	95
12	Probabilistic methods (Bayesian methods, variational inference, sampling, UQ, etc.)	220
13	Applications to robotics, autonomy, planning	196
14	Learning on graphs and other geometries & topologies	320
15	Societal considerations including fairness, safety, privacy	214
16	Optimization	328
17	Visualization or interpretation of learned representations	87
18	Metric learning, kernel learning, and sparse coding	6
19	Infrastructure, software libraries, hardware, systems, etc.	50
20	Applications to computer vision, audio, language, and other modalities	574
21	Alignment, fairness, safety, privacy, and societal considerations	499
22	Interpretability and explainable AI	249
23	Foundation or frontier models, including LLMs	670
24	Learning on time series and dynamical systems	116
25	Other topics in machine learning (i.e., none of the above)	223

1107

1108

The top-left $n \times n$ block equals $\text{Diag}(z_1, \dots, z_n) - M^+B$, whose determinant is a nonzero polynomial (the $z_1 \dots z_n$ coefficient equals 1), hence it is invertible for almost all z_c ; thus $D\varphi_o(z_c)$ is invertible generically. There exists (up to scale) a unique nonzero w with

1111

1112

1113

1114

1115

1116

$$w^\top \left(\begin{pmatrix} z_1 & 0 & \cdots & 0 \\ \ddots & \ddots & & \vdots \\ 0 & \cdots & z_n & 0 \\ 0 & \cdots & 0 & 0 \end{pmatrix} - \tilde{M}^+B \right) = 0, \quad w^\top \left(\begin{pmatrix} \tilde{z}_1 & 0 & \cdots & 0 \\ \ddots & \ddots & & \vdots \\ 0 & \cdots & \tilde{z}_n & 0 \\ 0 & \cdots & 0 & 0 \end{pmatrix} - \tilde{M}^+B \right) = 0. \quad (34)$$

1117

If some w_i vanished on a set of positive measure, either the upper block would lose rank (contradicting the generic invertibility) or a minor involving the bottom row would force $(v^\top B)_1 = 0$, violating Assumption ii. Hence $w_i \neq 0$ for all $i \leq n$ almost everywhere, and subtracting the two displays gives

1118

1119

$$(w_1(z_1 - \tilde{z}_1), \dots, w_n(z_n - \tilde{z}_n), 0) = 0, \quad (35)$$

1120

1121

1122

1123

so $z_i = \tilde{z}_i$ for all $1 \leq i \leq n$. Therefore $\varphi_o(z_c) = z_c$ almost everywhere (and by continuity everywhere), which implies

1124

1125

$$\langle e_i, \tilde{g}^{-1}(x) \rangle = \langle e_i, g^{-1}(x) \rangle, \quad 1 \leq i \leq n. \quad (36)$$

1126

1127

1128

Thus the concept coordinates, hence the true concepts $\mathbf{c} = A\mathbf{z}$, are identified up to permutation and coordinate-wise scaling. Since $\tilde{\mathbf{c}}$ enters only as weak supervision with independent Gaussian noise, it does not alter the identifiability class of \mathbf{c} ; rather, it guides estimation.

1129

This completes the proof of Theorem 1.

1130

1131

1132

1133

1134

Prompt 1. (Complete Prompt for Generating Concepts for Authors/Reviewers (1/2))

1135

Task Description

1136 You are an expert analyst tasked with evaluating an author-reviewer discussion from the OpenReview system. Your goal is to label the
 1137 discussion content across 10 specific dimensions, as defined below, based on the provided reviewer comments, author rebuttals, and any
 1138 additional interactions. For each dimension, assign a score (1, 2, 3, 4, or 5) according to the calibration criteria provided, and provide a brief
 1139 justification (1-2 sentences) explaining your reasoning. This rubric is calibrated for top-tier machine learning conferences. A score of 3 reflects
 1140 the expected standards from competent researchers at a top conference. Scores of 1-2 indicate responses that fall short of this benchmark,
 1141 while 4-5 are reserved for rebuttals that are truly exceptional. Don't hesitate to give a 3 for strong, competent responses; use higher scores
 1142 only for standout cases. Ensure your analysis is objective, precise, and grounded in the content.

1143

Input Content:

1144 The discussion content is provided in JSON format, containing reviewer summaries, strengths, weaknesses, questions, ratings, and author
 1145 responses. Here is the content with one reviewer's comments to analyze:

1146

{discussion}

1147

Dimensions and Calibration Criteria:

1148

1. Clarity of the Rebuttal (Presentation)

1149 Definition: The extent to which the rebuttal communicates the authors' arguments and clarifications clearly, with logical structure, precise
 language, and proper grammar.

Calibration:

1150

- 1 (Weak): Generally understandable but with notable ambiguity or unclear phrasing.
- 2 (Acceptable): Mostly clear, but with occasional awkwardness or minor lapses in flow or precision.
- 3 (Competent): Well-structured and precise, meeting top-tier expectations.
- 4 (Strong): Exceptionally clear and engaging, with polished language and logical flow.
- 5 (Exceptional): Exemplary clarity using outstanding prose or innovative formatting to enhance understanding.

1151

2. Directness in Addressing Reviewer Concerns (Presentation)

1152 Definition: The degree to which the rebuttal directly and comprehensively responds to the reviewer's specific criticisms and questions.

Calibration:

1153

- 1 (Inadequate): Fails to meaningfully engage with reviewer concerns.
- 2 (Partially Direct): Responds to some points but omits or glosses over others.
- 3 (Fully Direct): Addresses all major concerns clearly and completely.
- 4 (Very Direct): Thoughtful, complete, and anticipates follow-ups.
- 5 (Exceptionally Direct): Insightful, persuasive, and goes beyond expectations in addressing concerns.

1154

3. Positive Attitude (Presentation)

1155 Definition: The extent to which the rebuttal maintains a constructive, respectful, and collaborative tone, even when disagreeing with reviewers.

Calibration:

1156

- 1 (Negative): Dismissive or combative tone.
- 2 (Slightly Defensive): Polite but subtly frustrated or curt.
- 3 (Constructive): Respectful, professional, and collaborative.
- 4 (Gracious): Appreciative and collegial, fostering a positive tone.
- 5 (Diplomatic): Extremely professional and generous in tone, even under criticism.

1157

4. Willingness to Acknowledge Limitations or Propose Changes (Presentation)

1158 Definition: The authors' openness to revising their work and candidly acknowledging limitations raised by reviewers.

Calibration:

1159

- 1 (Resistant): Avoids or dismisses valid concerns.
- 2 (Minimally Open): Acknowledges minor issues with superficial fixes.
- 3 (Open): Candidly acknowledges limitations and proposes improvements.
- 4 (Receptive): Actively proposes meaningful adjustments.
- 5 (Reflective): Embraces feedback and suggests substantial changes with humility.

1160

5. Strength of Evidence or Justification (Technical)

1161 Definition: The robustness of the rebuttal's claims, supported by experiments, references, logical reasoning, or other concrete evidence.

Calibration:

1162

- 1 (Weak): Vague or unsupported claims.
- 2 (Partially Supported): Limited or insufficient justification.
- 3 (Well Justified): Solid and relevant evidence or logic.
- 4 (Thorough): Multiple, well-integrated forms of support.
- 5 (Persuasive): Deep, compelling evidence demonstrating technical mastery.

1163

6. Technical Convincingness and Rigor (Technical)

1164 Definition: The technical soundness, rigor, and depth of understanding demonstrated in the rebuttal's arguments.

Calibration:

1165

- 1 (Unconvincing): Contains technical errors or vague reasoning.
- 2 (Partially Convincing): Shows some understanding but includes logical gaps.
- 3 (Solid and Sound): Technically correct and well-reasoned.
- 4 (Insightful): Demonstrates thoughtful, deeper understanding.
- 5 (Exceptional): Reveals technical mastery and strengthens the paper's core claims.

1166

1167

1168

1169

1188
1189**Prompt 2. (Complete Prompt for Generating Concepts for Authors/Reviewers (2/2))****7. Handling of Misunderstandings and De-escalation***Definition: The extent to which the authors recognize and address misunderstandings in reviewer comments while maintaining a constructive tone.**Calibration:*

- 1 (Defensive): Escalates tension with sarcasm or dismissiveness.
- 2 (Tense): Curt or irritated tone; misunderstanding remains partially unresolved.
- 3 (Professional): Clarifies misunderstandings calmly and clearly.
- 4 (Tactful): Resolves issues gracefully and respectfully.
- 5 (Masterful): Turns conflict into constructive dialogue with diplomacy.

8. Review Specificity and Constructiveness*Definition: The specificity, actionability, and constructiveness of the reviewer's feedback provided to the authors.**Calibration:*

- 1 (Vague): Lacks actionable suggestions.
- 2 (Somewhat Specific): Contains some helpful points but is mixed with generalities.
- 3 (Constructive): Clear, specific, and actionable feedback.
- 4 (Thorough): Covers various aspects with a balanced and helpful tone.
- 5 (Exemplary): Deeply engaged, precise, and improvement-oriented feedback.

9. Reviewer Open-mindedness*Definition: The reviewer's apparent willingness to reconsider their evaluation based on a compelling rebuttal.**Calibration:*

- 1 (Rigid): Unwilling to engage or revise stance.
- 2 (Cautious): Skeptical, with minimal openness.
- 3 (Reasonable): Acknowledges merit and shows willingness to revise.
- 4 (Flexible): Thoughtfully re-evaluates if rebuttal is persuasive.
- 5 (Proactive): Encourages rebuttal and signals readiness to change stance.

10. Severity of Concerns*Definition: The seriousness of the reviewer's criticisms, influencing the rebuttal's potential to change the reviewer's opinion.**Calibration:*

- 1 (Minor): Only minor or editorial comments.
- 2 (Moderate): Substantive but addressable issues.
- 3 (Serious): Challenges to key aspects of the paper.
- 4 (Major): Foundational doubts about core contributions.
- 5 (Critical): Calls the publishability of the work into question.

Instructions

1. Analyze the provided content, focusing on the author's rebuttal (if any) and the reviewer's comments.
2. For each of the 10 dimensions, assign a score (1, 2, 3, 4, or 5) based on the calibration criteria.
3. Provide a brief justification (1-2 sentences) for each score, referencing specific aspects of the content.
4. **Summary:** After analyzing all, provide a summary string containing the 10 dimension scores separated by hyphens.
5. If a dimension cannot be evaluated due to insufficient information (e.g., no rebuttal for technical dimensions), assign a score 0 and explain why.
6. If the content references another reviewer (e.g., "reviewer ciFG" or "reviewer sq8T") whose comments are not provided, note that the analysis is limited to the available content.
7. Ensure your tone remains neutral and professional, focusing on the content's quality and alignment with the criteria.
8. Present your output strictly in the following format:

Output Format

1. **Clarity of the Rebuttal:** [Score]
Justification: [1-2 sentences]
2. **Directness in Addressing Reviewer Concerns:** [Score]
Justification: [1-2 sentences]
3. **Positive Attitude:** [Score]
Justification: [1-2 sentences]
4. **Willingness to Acknowledge Limitations or Propose Changes:** [Score]
Justification: [1-2 sentences]
5. **Strength of Evidence or Justification:** [Score]
Justification: [1-2 sentences]
6. **Technical Convincingness and Rigor:** [Score]
Justification: [1-2 sentences]
7. **Handling of Misunderstandings and De-escalation:** [Score]
Justification: [1-2 sentences]
8. **Review Specificity and Constructiveness:** [Score]
Justification: [1-2 sentences]
9. **Reviewer Open-mindedness:** [Score]
Justification: [1-2 sentences]
10. **Severity of Concerns:** [Score]
Justification: [1-2 sentences]

Summary: [Score1-Score2-...-Score10].

Figure A3: Conditional Independence Test. The p-value of KCI (blue) and RCIT (orange).

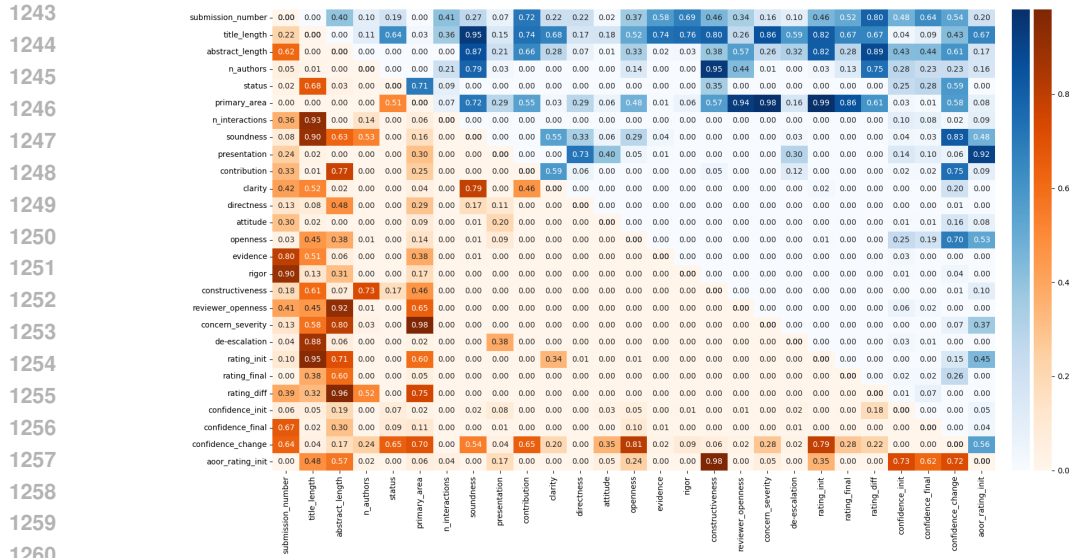


Figure A4: Conditional Independence Test. The p-value of HSIC (blue) and Chi-square (orange).

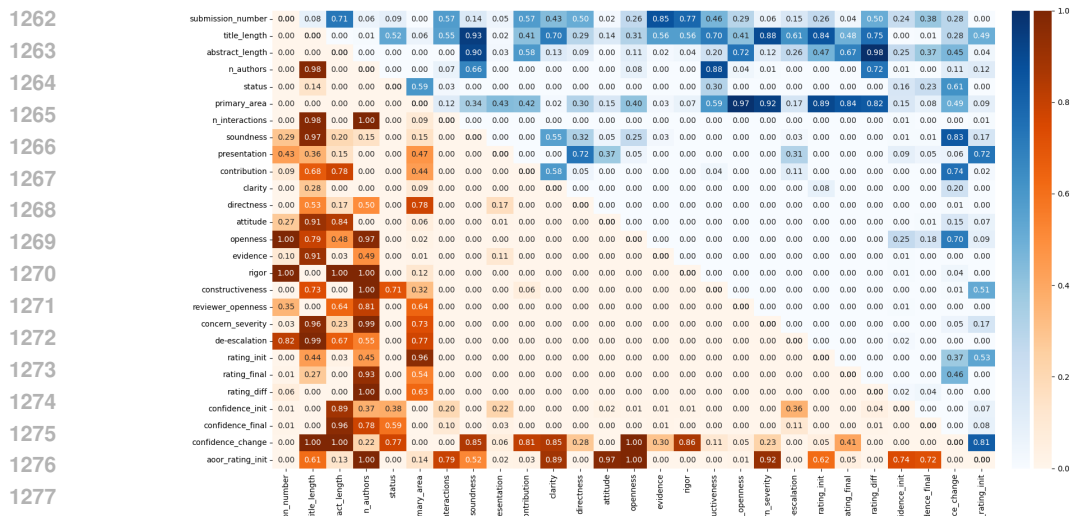
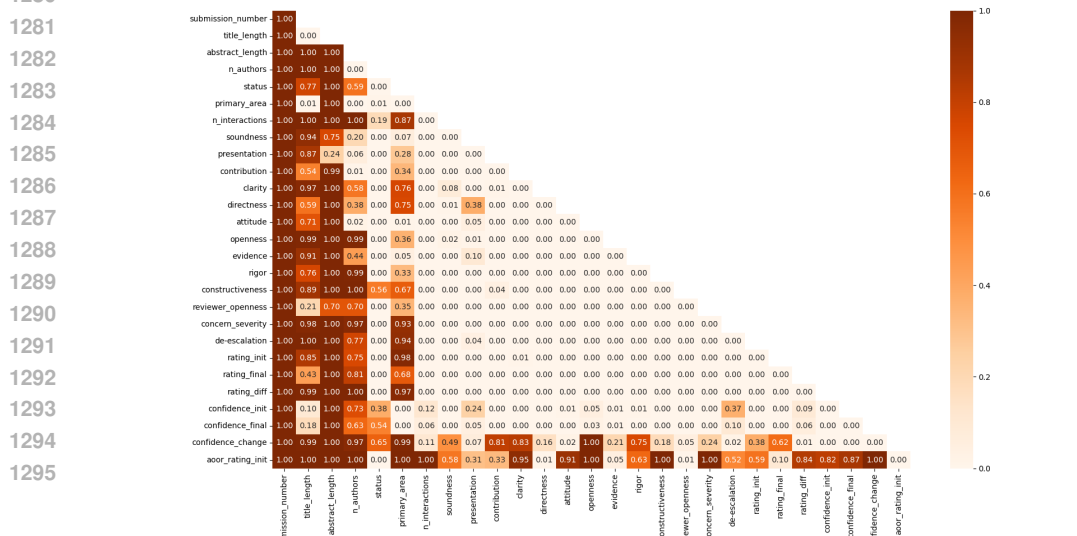


Figure A5: Conditional Independence Test. The p-value of GSQ (orange).



1296

1297

1298

1299

1300

1301

1302

1303

1304

1305

1306

1307

1308

1309

1310

1311

1312

1313

1314

1315

1316

1317

1318

1319

1320

1321

1322

1323

1324

1325

1326

1327

1328

1329

1330

1331

1332

1333

1334

1335

1336

1337

1338

1339

1340

1341

1342

1343

1344

1345

1346

1347

1348

1349

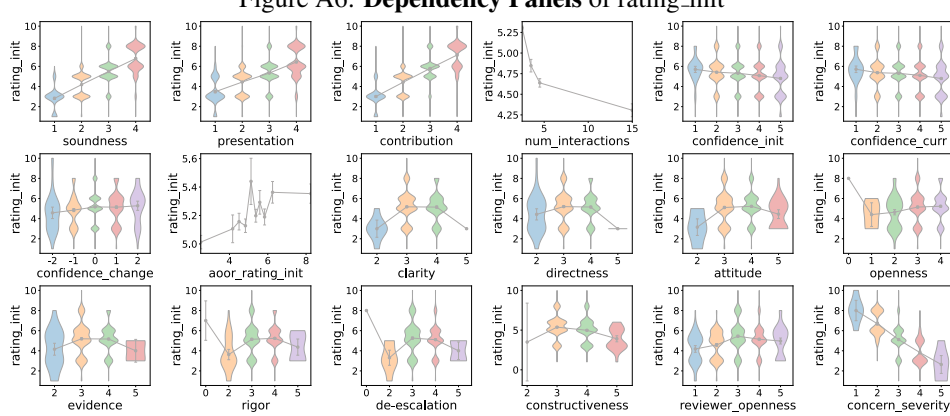


Figure A6: Dependency Panels of rating_init

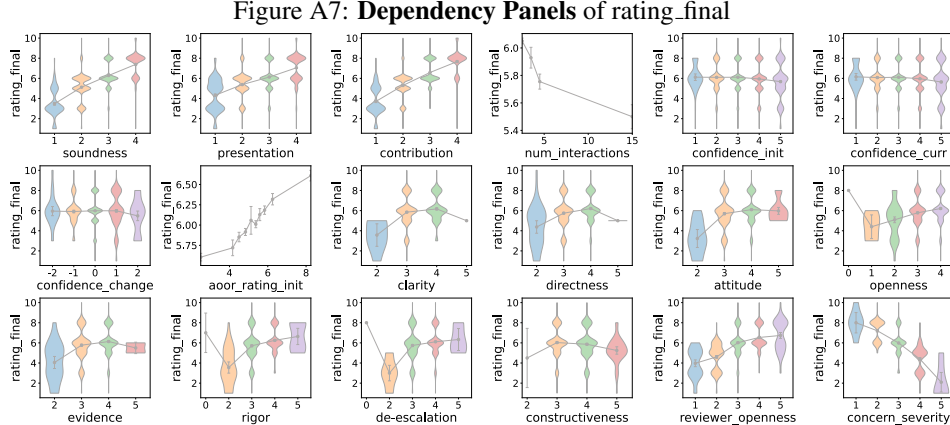


Figure A7: Dependency Panels of rating_final